ELSEVIER

Advances in Environmental Research 4 (2000) 187–209

Advances in Environmental Research

www.elsevier.nl/locate/aer

A numerical model simulating reactive transport in shallow water domains: model development and demonstrative applications

H.-P. Cheng[a,*], G.-T. Yeh[b], J.-R. Cheng[c]

[a] *Department of Nuclear Science, National Tsing Hua University, Hsinchu, Taiwan 300, R.O.C.*
[b] *Department of Civil and Environmental Engineering, The Pennsylvania State University, University Park, PA 16802, USA*
[c] *Department of Computer Science and Engineering, The Pennsylvania State University, University Park, PA 16802, USA*

Accepted 27 March 2000

Abstract

We present a two-dimensional depth-averaged numerical model simulating reactive transport in shallow water domains subject to given flow conditions. A new approach is used to account for more conceivable kinetically-controlled chemical reactions than have been included in previous models. In this model, a chemical may dissolve in the water column or in the interstitial water of the bed sediments, react with other dissolved chemicals to form new chemicals also in the dissolved phase, or be sorbed onto sediments to become particulate chemicals. To save computer time, we employ a predictor–corrector strategy to deal with the reactive transport equations of mobile substances where transport equations are computed in the predictor step with reaction rates estimated at the previous time step, and rate correction is achieved node by node in the corrector step to obtain the concentration distributions at the present time step. For immobile substances, we solve the corresponding ordinary differential equations together with the corrector equations of mobile substances in the corrector step by using the Newton–Raphson method. Two examples are demonstrated to show the capability of our model.

Keywords: Reactive transport; Shallow water domain; Numerical simulation

1. Introduction

With increasing comprehension worldwide of all aspects of environmental and ecological pollution in bay/estuary areas, many scientists and engineers have devoted themselves to the study of environmental impact analysis/assessment. Some environmental considerations relating to water pollution and sediment transport, such as low dissolved oxygen, eutrophication, retention time, flushing efficiency, and erosion/deposition, have been brought into these studies. Falconer has listed many potential contaminant sources causing water pollution in bay/estuary areas (Falconer, 1990). Because of the rapid development of computer technology and many restrictions associated with physical

* Corresponding author. Tel.: +886-3-574-5831; fax: +886-3-574-5831.

E-mail addresses: hpcheng@mx.nthu.edu.tw (H.-P. Cheng), gty2@psu.edu (G.-T. Yeh), jccheng@cse.psu.edu (J.-R. Cheng).

1093-0191/00/$ - see front matter
PII: S1093-0191(00)00015-0

models, e.g. scaling and distortion, cost, inflexibility, lack of transportability and adaptability (Falconer, 1992), there has been a marked increase in the development and application of numerical models to predict water quality indicators and sediment distribution changes in estuarine waters in recent years.

Applications of water quality models mainly included studies of chemical distributions (Sheng et al., 1995a; Blumberg et al., 1996; Paulsen and Owen, 1996; Falconer and Lin, 1997) and sediment distributions (McDonald and Cheng, 1994; Sheng et al., 1995b; Paulsen and Owen, 1996) through natural or man-induced injections. To improve computational accuracy and efficiency, a variety of numerical strategies have been proposed, such as the splitting method (Sommeijer and Kok, 1996; Falconer and Lin, 1997), upwind formulation (Sommeijer and Kok, 1996; Falconer and Lin, 1997; Ors, 1997); the Lagrangian–Eulerian (LE) approach (Wood and Baptista, 1992; Hinkelmann and Zielke, 1996; Spitaleri and Corinaldesi, 1997), the parallel method (Hinkelmann and Zielke, 1996), and a decoupling scheme (Park and Kuo, 1996). Many models account for only conservative substances and the corresponding governing equations are typical advection–dispersion transport equations. Others consider non-conservative constituents by taking into account either first-order reaction kinetics or partitioning between aqueous and solid phases (Park and Kuo, 1996; Paulsen and Owen, 1996; Falconer and Lin, 1997).

Although numerical approaches have been intensively studied, no existing water quality model, to our knowledge, has used a fully mechanistic approach to estimate non-conservative chemical transport in shallow water domains. All existing models are either empirically-based or simulate systems containing specific reactions. They may provide a very efficient monitoring and management tool because they are calibrated for specific environments. However, they are usually limited in the extent to which they can be applied to other systems. On the other hand, a model that considers interactions among chemicals based on fundamental reaction mechanisms and can be applied to all systems (Steefel and Cappellen, 1998). Although many of the reactions that take place in natural systems have not been clearly identified, and different formulations may be required for different rate constants, when adequately constructed such a model can be used to elucidate complex natural systems where the system behavior may be non-intuitive even when all the important processes have been identified. In addition, developing a more comprehensive model for a particular system, even if more complicated, offers the possibility of testing for multiple hypotheses (Steefel and Cappellen, 1998).

Based on our experience in modeling reactive transport in the subsurface (Yeh and Tripathi, 1990; Cheng and Yeh, 1998; Yeh et al., 1998), we present in this paper a numerical model simulating two-dimensional reactive transport in shallow water domains with an approach to account for more conceivable reactions than have been included in previous models. In our model, sediments are categorized based on their physical and chemical properties. For each category of sediment, we include suspended sediment particles scattered in the water column and bed sediment particles accumulated on the bed rock/soil. The distribution of suspended and bed sediments is controlled through hydrological transport as well as erosion and deposition processes. A chemical species, either organic or inorganic, may appear in the water column as a dissolved chemical, be sorbed onto a sediment to become a particulate chemical, or dissolve in the interstitial water of the bed sediment. All reactions among chemicals are assumed to be kinetic, and reaction rates are described based on the collision theory (Stumm and Morgan, 1981) where forward and backward rate constants are measured experimentally. Fig. 1 shows a schematic plot for the reactions taken into account in our model.

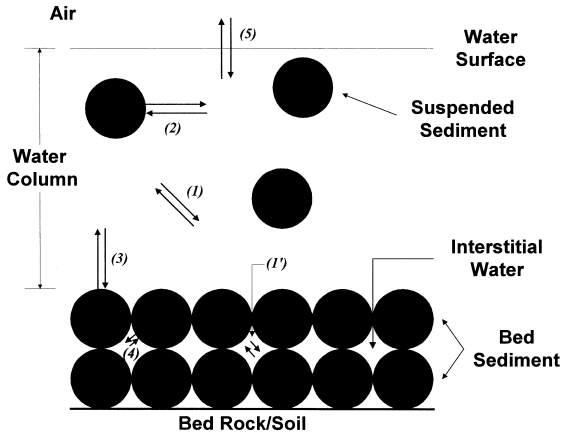

Fig. 1. Schematic plot of chemical reactions taken into account in the model. Reactions include (1 & 1′) aqueous complexation reactions in the water column and in the interstitial water; (2) adsorption/desorption between the water column and suspended sediments; (3) adsorption/desorption reactions between the water column and bed sediments; (4) adsorption/desorption reactions between the interstitial water and bed sediments; and (5) volatilization reactions between the water column and atmosphere.

In developing this model, we have assumed (1) flow fields are not influenced by sediment or contaminant distributions; and (2) sediment distributions are not affected by contaminant distributions. The first assumption gives our model the full flexibility to be linked with any two-dimensional finite element flow model which solves depth-averaged hydrodynamic equations. The second assumption allows us to calculate sediment transport prior to contaminant transport

in our numerical approach as will be described later on. In addition, temperature effects and density effects (Cheng and Yeh, 1998) are not considered in the current version of the model, but will be accounted for in a later version.

Theoretically, strong coupling (Cheng and Yeh, 1998) must be used to couple chemical reactions with physical transport to provide accurate solutions. This might, however, require many coupling iterations to reach convergence or even create convergence problems. To efficiently solve reactive contaminant transport equations, most subsurface reactive contaminant transport models employ operator splitting strategies to decouple solute transport from chemical reactions (Chilakapathi, 1995; Salvage, 1998) with a possibility of sacrificing accuracy to a significant degree (Salvage, 1998). Rather than operator splitting, we use a predictor–corrector scheme to effectively compute reactive contaminant transport without surrendering much accuracy when diffusion is not significant. We also employ the LE approach to deal with transport equations where a particle tracking technique (Cheng et al., 1996a) is applied in the Lagrangian step while the Galerkin finite element method is implemented in the Eulerian step.

We organize this paper as follows. We will first describe the governing equations and the associated initial and boundary conditions in Section 2, followed by the numerical approach in Section 3. We will use two example problems for demonstration in Section 4 and conclude this paper in Section 5.

2. Mathematical statement

The two-dimensional depth-averaged governing equations of transport in shallow water domains can be derived according to the conservation law of material mass and through the averaging process over water depth (Wang and Connor, 1975). In the model, suspended sediments, dissolved chemicals in the water column, and particulate chemicals on suspended sediments are subject to transport, while bed sediments, particulate chemicals on bed sediments, and dissolved chemicals in the interstitial water are considered immobile. The governing equations can be written as follows.

2.1. Continuity equations for suspended sediments: $n \in [1,N_s]$

$$\frac{\partial(hS_n)}{\partial t} + \nabla\cdot(\mathbf{q}S_n) = \nabla\cdot[h\mathbf{K}\cdot\nabla S_n] + M_n^s + (R_n - D_n) \tag{1}$$

where N_s is the number of sediment sizes; h is water depth $[L]$; t is time $[T]$; $\boldsymbol{q}$ is the flow flux $[L^2/T]$; ∇ is the del operator; S_n is the depth-averaged sediment concentration of the n-th fraction size in the water column $[M/L^3]$; $\boldsymbol{K}$ is the dispersion coefficient tensor $[L^2/T]$; M_n^s is the source of the n-th size fraction sediment $[M/L^2/T]$; R_n is the erosion rate of the n-th size fraction sediment $[M/L^2/T]$; D_n is the deposition rate of the n-th size fraction sediment $[M/L^2/T]$. The determination of D_n and R_n can be found elsewhere (Graf, 1984).

2.2. Continuity equations for bed sediments: $n \in [1,N_s]$

$$\frac{\partial M_n}{\partial t} = D_n - R_n \tag{2}$$

where M_n is the sediment mass per unit horizontal bed area of the n-th size fraction $[M/L^2]$.

2.3. Continuity equations for dissolved chemicals in the water column: $i \in [1,N_c]$

$$\begin{aligned}
&\frac{\partial(hC_i^w)}{\partial t} + \nabla\cdot(\mathbf{q}C_i^w) \\
&= \nabla\cdot[h\mathbf{K}\cdot\nabla C_i^w] + M_i^{cw} - \lambda_i^w h C_i^w + hk_i^{ab}\left(p_i - \frac{k_i^{af}}{k_i^{ab}}C_i^w\right) \\
&+ \sum_{n=1}^{N_s} k_{ni}^{sb} S_n h\left(C_{ni}^s - \frac{k_{ni}^{sf}}{k_{ni}^{sb}}C_i^w\right) \\
&+ \sum_{n=1}^{N_s} k_{ni}^{bb} M_n\left(C_{ni}^b - \frac{k_{ni}^{bf}}{k_{ni}^{bb}}C_i^w\right) \\
&+ \sum_{m=1}^{N_{rx}} (a_{mi} - b_{mi}) k_m^{rb} h\left[\prod_{j=1}^{N_c}(C_j^w)^{b}{}_{mj} - \frac{k_m^{rf}}{k_m^{rb}}\prod_{j=1}^{N_c}(C_j^w)^{a}{}_{mj}\right] \\
&- E(C_i^w - C_i^{bw}) - \left(\sum_{n=1}^{N_s}\frac{D_n}{\rho_n}\theta_n\right)C_i^w + \left(\sum_{n=1}^{N_s}\frac{R_n}{\rho_n}\theta_n\right)C_i^{bw}
\end{aligned} \tag{3}$$

where N_c is the number of dissolved chemicals; C_i^w is the depth-averaged concentration of the i-th dissolved chemical in the water column $[M/L^3]$; M_i^{cw} is the source of the i-th dissolved chemical $[M/L^2/T]$; λ_i^w is the combined first-order degradation rate constant of the i-th dissolved chemical $[1/T]$; k_i^{ab} and k_i^{af} are the backward and the forward volatilization rate constants, respectively, associated with the i-th dissolved chemical in the atmosphere; p_i is the partial pressure in the

atmosphere associated with the i-th dissolved chemical [atm]; k_{ni}^{sb} and k_{ni}^{sf} are the backward and the forward sorption rate constants, respectively, associated with the i-th particulate chemical on suspended sediment of the n-th fraction size; C_{ni}^{b} is the mass of particulate chemical on unit mass of bed sediment of the n-th fraction size $[M/M]$; k_{ni}^{bb} and k_{ni}^{bf} are the backward and the forward sorption rate constants, respectively, associated with the i-th particulate chemical on bed sediment of the n-th fraction size; C_{ni}^{s} is the mass of particulate chemical on unit mass of suspended sediment of the n-th fraction size $[M/M]$; N_{rx} is the number of aqueous complexation reactions; k_{m}^{rb} and k_{m}^{rf} are the backward and forward rate constants, respectively, of the m-th aqueous complexation reaction; a_{mj} (b_{mj}) is the stoichiometric coefficient of the j-th dissolved chemical in the m-th aqueous complexation reaction when this dissolved chemical appears as a reactant (product) chemical; C_{i}^{bw} is the concentration of the i-th dissolved chemical in the interstitial water $[M/L^3]$; θ_n is the porosity of the n-th size fraction bed sediment; ρ_n is the bulk density of the n-th size bed sediment $[M/L^3]$; E is the exchange coefficient between the interstitial water of bed sediments and the water in the water column $[L^3/L^2/T]$, which can be determined experimentally. In Eq. (3), the first term on the left side represents the mass increase rate of a dissolved chemical per unit horizontal area, while the second term on the left is the advection transport term. On the right-hand-side of Eq. (3), the first term is the dispersion transport term, the second is the external source, the third represents an overall first-order decay, the fourth is from the volatilization reactions, the fifth and the sixth are from the reactions of sorption/desorption between the water column and suspended sediments and between the water column and bed sediments, respectively, the seventh is from the aqueous complexation reactions in the water column, the eighth is the exchange between the water column and the interstitial water due to diffusion, the ninth and tenth are the physical exchanges between the water column and the interstitial water due to deposition and erosion, respectively.

2.4. Continuity equations for particulate chemicals on suspended sediments: $n \in [1,N_s]$, $i \in [1,N_c]$

$$\begin{aligned}&\frac{\partial(hS_nC_{ni}^{s})}{\partial t}+\nabla\cdot(\mathbf{q}S_nC_{ni}^{s})\\&=\nabla\cdot[h\mathbf{K}\cdot\nabla(S_nC_{ni}^{s})]+M_{ni}^{cs}-\lambda_{ni}^{s}hS_nC_{ni}^{s}\\&-k_{ni}^{sb}S_nh\left(C_{ni}^{s}-\frac{k_{ni}^{sf}}{k_{ni}^{sb}}C_{i}^{w}\right)+R_nC_{ni}^{b}-D_nC_{ni}^{s}\end{aligned}\tag{4}$$

where M_{ni}^{cs} is the source of the i-th particulate chemical on suspended sediment of the n-th fraction size $[M/L^2/T]$; λ_{ni}^{s} is the combined first-order degradation rate constant of the i-th particulate chemical on suspended sediment of the n-th fraction size $[1/T]$. In Eq. (4), the first term on the left side represents the rate of mass increase of a suspended particulate chemical per unit horizontal area, while the second term on the left is the advection transport term. On the right-hand-side, the first term is the dispersion transport term, the second is the external source, the third represents an overall first-order decay, the fourth is from the reactions of sorption/desorption between the water column and suspended sediments, the fifth is due to erosion, and the last is due to deposition.

2.5. Continuity equations for particulate chemicals on bed sediments: $n \in [1,N_s]$, $i \in [1,N_c]$

$$\begin{aligned}\frac{\partial(M_nC_{ni}^{b})}{\partial t}&=(D_nC_{ni}^{s}-R_nC_{ni}^{b})-\lambda_{ni}^{b}M_nC_{ni}^{b}\\&-k_{ni}^{bb}M_n\left[C_{ni}^{b}-\frac{k_{ni}^{bf}}{k_{ni}^{bb}}C_{i}^{w}\right]+k_{ni}^{2f}M_nC_{i}^{bw}\\&-k_{ni}^{2b}M_nC_{ni}^{b}\end{aligned}\tag{5}$$

where λ_{ni}^{b} is the combined first-order degradation rate constant of the i-th particulate chemical on bed sediment of the n-th fraction size $[1/T]$. In the above equation, the term on the left side represents the rate of mass increase of a bed particulate chemical per unit horizontal area. The first and second terms on the right side of the equation are due to deposition and erosion, respectively, the third represents an overall first-order decay, the fourth is from the reactions of sorption/desorption between the water column and bed sediments, and the fifth and sixth are from the reactions of sorption/desorption between the interstitial water and bed sediments.

2.6. Continuity equations for dissolved chemicals in the interstitial water: $n \in [1,N_s]$, $i \in [1,N_c]$

$$\begin{aligned}&\frac{\partial\left(\sum_{n=1}^{N_s}\frac{\theta_n}{\rho_n}M_nC_{i}^{bw}\right)}{\partial t}\\&=E(C_{i}^{w}-C_{i}^{bw})+\sum_{n=1}^{N_s}\frac{D_n}{\rho_n}\theta_n(C_{i}^{w}-C_{i}^{bw})\\&-\sum_{n=1}^{N_s}(k_{ni}^{2f}M_nC_{i}^{bw}-k_{ni}^{2b}M_nC_{ni}^{b})\end{aligned}$$

$$+\left(\sum_{n=1}^{N_s}\frac{\theta_n}{\rho_n}M_n\right)\sum_{m=1}^{N_{rx}}(a_{mi}-b_{mi})$$
$$\times k_m^{rb}\left[\prod_{j=1}^{N_c}\left(C_j^{bw}\right)^{b}{}_{mj}-\frac{k_m^{rf}}{k_m^{rb}}\prod_{j=1}^{N_c}\left(C_j^{bw}\right)^{a}{}_{mj}\right] \quad (6)$$

where k_{ni}^{2b} and k_{ni}^{2f} are the backward and the forward sorption rate constants, respectively, associated with the i-th particulate chemical in the interstitial water of bed sediment of the n-th fraction size. In Eq. (6), the term on the left side represents the mass increase rate of a dissolved chemical in the interstitial water per unit horizontal area. The first term on the right side is due to diffusion between the water column and the interstitial water, the second is from deposition, the third is from the reactions of sorption/desorption between the water column and bed sediments, and the last is from the aqueous complexation reactions in the interstitial water.

In constructing Eqs. (3)–(6), the following reactions are considered.

2.7. Aqueous complexation reactions in the water column and in the interstitial water: $m \in [1,N_{rx}]$

$$\sum_{i=1}^{N_c}a_{mi}\mathbf{C_i}\rightleftarrows\sum_{i=1}^{N_c}b_{mi}\mathbf{C_i} \quad (7)$$

$$R_a=k_m^{rf}\prod_{i=1}^{N_c}(C_i)^{a}{}_{mi}-k_m^{rb}\prod_{i=1}^{N_c}(C_i)^{b}{}_{mi} \quad (8)$$

where C_i can be either C_i^w or C_i^{bw}; R_a is defined as the rate of the aqueous complexation reaction.

2.8. Sorption / desorption reactions between the water column and suspended sediments: $n \in [1,N_s]$, $i \in [1,N_c]$

$$\mathbf{C_i^w}+\mathbf{S_n}\rightleftarrows\mathbf{C_{ni}^s}+\mathbf{S_n} \quad (9)$$

$$R_{ad}^{s}=k_{ni}^{sf}S_nC_i^w-k_{ni}^{sb}S_nC_{ni}^s \quad (10)$$

where R_{ad}^{s} is defined as the rate of the sorption reaction.

2.9. Sorption / desorption reactions between the water column and bed sediments: $n \in [1,N_s]$, $i \in [1,N_c]$

$$\mathbf{C_i^w}+\mathbf{M_n}\rightleftarrows\mathbf{C_{ni}^b}+\mathbf{M_n} \quad (11)$$

$$R_{ad}^{b1}=k_{ni}^{bf}M_nC_i^w-k_{ni}^{bb}M_nC_{ni}^b \quad (12)$$

where R_{ad}^{b1} is defined as the rate of the sorption reaction.

2.10. Sorption / desorption reactions between interstitial water and bed sediments: $n \in [1,N_s]$, $i \in [1,N_c]$

$$\mathbf{C_i^{bw}}+\mathbf{M_n}\rightleftarrows\mathbf{C_{ni}^b}+\mathbf{M_n} \quad (13)$$

$$R_{ad}^{b2}=k_{ni}^{2f}M_nC_i^{bw}-k_{ni}^{2b}M_nC_{ni}^b \quad (14)$$

where R_{ad}^{b2} is defined as the rate of the sorption reaction.

2.11. Volatilization reactions between the water column and atmosphere: $i \in [1,N_c]$

$$\mathbf{C_i^w}\rightleftarrows\mathbf{p_i} \quad (15)$$

$$R_v=k_i^{af}C_i^w-k_i^{ab}p_i \quad (16)$$

where R_v is defined as the rate of the volatilization reaction. In Eqs. (7), (9), (11), (13) and (15) the bold form is used to represent the chemical formula of a contaminant or a sediment. It is noted that it is impossible to include all types of reactions, whether mechanism- or empiricism-based (e.g. reactions described by the Michaelis–Menton formulation), in our model. But once they are identified, they can be easily added to the governing equations as source/sink terms. The strategy for solving the governing equations remains the same as will be stated in Section 3.

To achieve transient simulations, the concentrations of contaminants and sediments must be provided initially. Five types of boundary conditions can be used for mobile substances, i.e. suspended sediments, dissolved chemicals, and particulate chemicals on suspended sediments. They are:

2.11.1. Dirichlet boundary condition

This condition is applied when concentration is given at a boundary. That is,

$$C(x_b,y_b,t)=C_b(t) \quad (17)$$

where C can be the S_n, C_i^w, or $S_nC_{ni}^s$; $C_b(t)$ is a prescribed time-dependent concentration on the boundary $[M/L^3]$.

2.11.2. Variable boundary condition

This boundary condition is employed when the flow direction changes with time during simulations. Two cases are considered with regard to the flow direction on the boundary segment.

2.11.2.1. < Case 1 > Flow is coming in from outside.

$$-\mathbf{n}\cdot[\mathbf{q}C(x_b,y_b,t)-h\mathbf{K}\cdot\nabla C(x_b,y_b,t)]=-\mathbf{n}\cdot\mathbf{q}C_{\text{in}}(t) \tag{18}$$

2.11.2.2. < Case 2 > Flow is going out from inside.

$$\mathbf{n}\cdot(-h\mathbf{K}\cdot\nabla C(x_b,y_b,t))=0 \tag{19}$$

where $\boldsymbol{n}$ is the outward unit normal vector of the boundary segment; $\boldsymbol{q}$ is the flow flux vector $[L^2/T]$; $\boldsymbol{K}$ is the dispersion coefficient tensor $[L^2/T]$; $C_{\text{in}}(t)$ is the prescribed time-dependent concentration $[M/L^3]$, associated with the incoming flow.

2.11.3. Ocean boundary condition

This boundary condition is employed when the flow is controlled by tides. Two cases are considered again with regard to the flow direction on the boundary segment.

2.11.3.1. < Case 1 > Flow is coming in from outside.

$$-\mathbf{n}\cdot[\mathbf{q}C(x_b,y_b,t)-h\mathbf{K}\cdot\nabla C(x_b,y_b,t)]=-\mathbf{n}\cdot\mathbf{q}C_o(t) \tag{20}$$

2.11.3.2. < Case 2 > Flow is going out from inside.

$$\mathbf{n}\cdot(-h\mathbf{K}\cdot\nabla C(x_b,y_b,t))=0 \tag{21}$$

where $C_o(t)$, a prescribed time-dependent concentration $[M/L^3]$ at the ocean boundary during the incoming flow, will be specified as

$$C_o(t)=C_{\max}e^{-ft} \tag{22}$$

where $C_{\max}$ is the maximum concentration at the end of the last outgoing flow and f is a flushing decay constant, which is estimated to match the specific flushing rate obtained from field data.

2.11.4. Cauchy boundary condition

This condition is applied when the total incoming material flux is prescribed as a function of time on a boundary segment. It can be written as

$$-\mathbf{n}\cdot[qC(x_b,y_b,t)-h\mathbf{K}\cdot\nabla C(x_b,y_b,t)]=q_b^c(t) \tag{23}$$

where $q_b^c(t)$ is a prescribed time-dependent Cauchy flux $[M/T/L]$.

2.11.5. Neumann boundary condition

This condition is employed when the incoming diffusive material flux can be prescribed on a boundary segment. It is written as

$$-\mathbf{n}\cdot(-h\mathbf{K}\cdot\nabla C(x_b,y_b,t))=q_b^n(t) \tag{24}$$

where $q_b^n(t)$ is a prescribed time-dependent Neumann flux $[M/T/L]$.

3. Numerical approach

In shallow water domains where advection dominates diffusion, the LE approach (Wood and Baptista, 1992) has been considered an appropriate way to compute material transport because it may greatly reduce many types of numerical error (Yeh, 1990). This approach guarantees non-negative computed concentration in solving solute transport equations when linear or bi-linear elements are used for discretization, which is required in computing concentration distributions subject to chemical reactions (Cheng and Yeh, 1998). Therefore, we can write the governing equations of mobile substances in the LE form as follows.

3.1. For suspended sediments: $n \in [1,N_s]$

$$h\frac{\mathrm{d}S_n}{\mathrm{d}t}-\nabla[\cdot h\mathbf{K}\cdot\nabla S_n]=[M_n^s+R_n-D_n]-SS_n \tag{25}$$

where $\mathrm{d}/\mathrm{d}t$ represents the material or total derivative with respect to time; S is the external fluid source $[L/T]$.

3.2. For dissolved chemicals in the water column: $i \in [1,N_c]$

$$\begin{aligned}h\frac{\mathrm{d}C_i^w}{\mathrm{d}t}-\nabla\cdot[h\mathbf{K}\cdot\nabla C_i^w]=&\sum_{m=1}^{N_{rx}}(a_{mi}-b_{mi})k_m^{rb}h\\&\times\left[\prod_{j=1}^{N_c}(C_j^w)_D mj^b-\frac{k_m^{rf}}{K_m^{rb}}\prod_{j=1}^{N_c}(C_j^w)^{a_{mj}}\right]\\&+\left[M_i^{cw}+hk_i^{ab}p_i+\sum_{n=1}^{N_s}k_{ni}^{sb}h(S_nC_{ni}^s)+\sum_{n=1}^{N_s}\right.\\&\left.\times\,k_{ni}^{bb}(M_nC_{ni}^b)+M_i^{crw}+EC_i^{bw}+\sum_n\frac{R_n}{\rho_n}\theta_nC_i^{bw}\right]\\&-\left[\lambda_i^wh+hk_i^{af}+\sum_{n=1}^{N_s}S_nhk_{ni}^{sf}+\sum_{n=1}^{N_s}M_nk_{ni}^{bf}+E\right.\\&\left.+\sum_n\frac{D_n}{\rho_n}\theta_n+S\right]C_i^w\end{aligned} \tag{26}$$

3.3. For particulate chemicals on suspended sediments: $n \in [1,N_s]$, $i \in [1,N_c]$

$$h\frac{\mathrm{d}(S_nC^s_{ni})}{\mathrm{d}t} - \nabla\cdot[h\mathbf{K}\cdot\nabla(S_nC^s_{ni})] = \left[M^{cs}_{ni} + k^{sf}_{ni}hS_nC^w_i + \frac{R_n}{M_n}(M_nC^b_{ni}) - \frac{D_n}{S_n}(S_nC^s_{ni})\right] - \left[\lambda^s_{ni}h + k^{sb}_{ni}h + S\right](S_nC^s_{ni}) \quad (27)$$

In obtaining Eqs. (25)–(27), we have substituted the flow continuity equation into Eqs. (1), (3) and (4). The flow continuity equation is the balance equation of water mass and can be written as follows.

$$\frac{\partial\eta}{\partial t} + \frac{\partial uh}{\partial x} + \frac{\partial vh}{\partial y} = S \quad (28)$$

where $\eta = \eta(x,y,t)$ is water surface elevation; u is the x-velocity $[L/T]$; v is the y-velocity $[L/T]$. Here we also define the water bed elevation $Z_0 = -d(x,y)$, where $d(x,y)$ is the water depth at mean water level. It is thus obvious that $\eta(x,y,t) = Z_0(x,y) + h(x,y,t)$ and $\partial\eta/\partial t = \partial h/\partial t$.

In solving Eqs. (25)–(27), we compute advection in the Lagrangian step where backward particle tracking is applied to determine the Lagrangian concentrations at all global nodes. We then use the Lagrangian concentrations as the initial conditions to solve the transport equations in the Eulerian step where the Galerkin finite element method is applied.

The two-dimensional transport equations presented above are a set of non-linear partial differential equations where non-linearity is introduced through the deposition/erosion and reaction terms. For the case in which diffusion is insignificant, we employ a predictor–corrector strategy to solve the governing equations to perform efficient computation without sacrificing much computational accuracy. Here we give a brief description of this strategy. The governing equations of mobile substances [i.e. Eqs. (25)–(27)] can be expressed in the following form.

$$h\frac{\mathrm{d}C}{\mathrm{d}t} = L(C) + \mathrm{RHS} \quad (29)$$

where C can be S_n, C^w_i, or $S_nC^s_{ni}$, L is the dispersion operator, and RHS represents other terms. With the predictor–corrector strategy, we solve Eq. (29) with the following two steps. First, we solve

$$h\frac{C^{N+1/2} - C^*}{\Delta\tau} = L(C^{N+1/2}) + (\mathrm{RHS})^N \quad (30)$$

where $\Delta\tau$ represents the time period consumed in backward particle tracking $[T]$; C^* is the Lagrangian concentration $[M/L^3]$; $(\mathrm{RHS})^N$ represents RHS evaluated at the previous time step $[M/L^2/T]$; $C^{N+1/2}$ is the intermediate concentration which we solve for with RHS evaluated at the previous time step $[M/L^3]$. It is noted that $\Delta\tau$ is the real time period for a fictitious particle to be advected from an upstream location to the global node being considered, and thus $\Delta\tau$ is location-dependent (Yeh et al., 1992). This time period is also what we use to calculate dispersion and reactions in the Eulerian step. Second, we solve

$$h\frac{C^{N+1} - C^*}{\Delta\tau} = L(C^{N+1/2}) + (\mathrm{RHS})^{N+1} \quad (31)$$

where C^{N+1} is the concentration of the present time step $[M/L^3]$; $(\mathrm{RHS})^{N+1}$ represents RHS evaluated at the present time step $[M/L^2/T]$. Subtracting Eq. (31) from Eq. (30) yields

$$h\frac{C^{N+1} - C^{N+1/2}}{\Delta\tau} = (\mathrm{RHS})^{N+1} - (\mathrm{RHS})^N \quad (32)$$

To save computer effort, we choose to solve Eq. (32) rather than Eq. (31) because Eq. (32) does not involve the dispersion operator and thus can be solved node by node. To summarize, we first solve Eq. (30) for $C^{N+1/2}$ in the predictor step, and then perform the corrector step by solving Eq. (32) to obtain C^{N+1}.

We employ an adaptive explicit–implicit scheme to avoid negative numerical results in solving Eq. (30). With this scheme, the following equation is actually solved when $(\mathrm{RHS})^N$ is negative.

$$h\frac{C^{N+1/2} - C^*}{\Delta\tau} - \frac{(\mathrm{RHS})^N}{C^N}C^{N+1/2} = L(C^{N+1/2}) \quad (33)$$

Consequently, we are solving the following correction equation in the corrector step.

$$h\frac{C^{N+1} - C^{N+1/2}}{\Delta\tau} = (\mathrm{RHS})^{N+1} - \frac{(\mathrm{RHS})^N}{C^N}C^{N+1/2} \quad (34)$$

With the Galerkin finite element approximation, Eq. (30) can be discretized as follows.

$$\left(\frac{[QA]}{\Delta\tau} + w[QD]\right)\{C\} = \frac{[QA]}{\Delta\tau}\{C^*\} + \{QR\} + (1-w)[QD]\{C^*\} + \{QB\} \quad (35)$$

where w is a time weighting factor; $[QA]$ is the mass matrix, $[QD]$ is the stiffness matrix due to dispersion;

$\{QR\}$ is the load vector contributed from $(\mathrm{RHS})^N$; and $\{QB\}$ is the load vector accounting for dispersive boundary fluxes. The associated element matrices and column vectors are defined as follows.

$$[QA]^e = \int_{R_e} N_i^e h N_j^e \mathrm{d}R_e \tag{36}$$

$$[QD]^e = \int_{R_e} \nabla N_i^e \cdot (h\mathbf{K} \cdot \nabla N_j^e) \mathrm{d}R_e \tag{37}$$

$$\{QR\}^e = \int_{R_e} N_i^e (\mathrm{RHS})^N \mathrm{d}R_e \tag{38}$$

$$\{QB\}^e = -\int_{B_e} N_i^e (-h\mathbf{K} \cdot \nabla C) \mathrm{d}B_e \tag{39}$$

where R_e and B_e represent the domain and the boundary, respectively, of element e; N_i^e and N_j^e are the element shape functions at the i-th and j-th element nodes, respectively, of element e. It is noted that $\{QR\}^e$ must be evaluated using nodal quadratures such that Eq. (30) and Eq. (32) are solved consistently. Also, boundary conditions for mobile substances are implemented in this predictor step. If $(\mathrm{RHS})^N$ is negative, Eq. (33) is solved in the predictor step. It can be discretized as

$$\left(\frac{[QA]}{\Delta\tau} + w[QD] - [QC]\right)\{C\} = \frac{[QA]}{\Delta\tau}\{C^*\} + (1-w)[QD]\{C^*\} + \{QB\} \tag{40}$$

where $[QC]$ is the stiffness matrix due to source/sink terms evaluated at the previous time step. The element matrix of $[QC]$ is defined as

$$[QC]^e = \int_{R_e} N_i \frac{(\mathrm{RHS})^N}{C^N} N_j \mathrm{d}R_e \tag{41}$$

where $[QC]^e$ must be lumped to maintain consistency in solving Eqs. (33) and (34).

With the predictor–corrector strategy, we solve the entire transport system by completing the following steps.

3.3.1. Step 1

We determine the Lagrangian concentrations for suspended sediments, dissolved chemicals in the water column, and particulate chemicals on suspend sediments, respectively.

3.3.2. Step 2

We solve Eqs. (25) and (2) for S_n and M_n, respectively. In this step, we first solve Eq. (25) with all source/sink terms evaluated at the previous time step to obtain the intermediate value for suspended sediments. Then we prepare the corrector form of Eq. (25) as follows.

$$h\frac{(S_n)^{N+1} - (S_n)^{N+1/2}}{\Delta\tau} = (\mathrm{RHS}_n^s)^{N+1} - (\mathrm{RHS}_n^s)^N \quad (\text{if } (\mathrm{RHS}_n^s)^N \geq 0)$$

$$= (\mathrm{RHS}_n^s)^{N+1} - \frac{(\mathrm{RHS}_n^s)}{(S_n)^N}(S_n)^{N+1/2} \ (\text{if } (\mathrm{RHS}_n^s)^N < 0) \tag{42}$$

where

$$(\mathrm{RHS}_n^s) = [M_n^s + R_n - D_n] - SS_n \tag{43}$$

At last, we solve Eqs. (42) and (2) node-by-node with the Picard method to obtain the solutions for suspended and bed sediments.

3.3.3. Step 3

We solve Eqs. (26), (27), (5) and (6) for C_i^w, $S_nC_{ni}^s$, $M_nC_{ni}^b$, and C_{ni}^{bw}, respectively. In this step, we solve Eqs. (26) and (27) with all source/sink terms evaluated at the previous time step to determine the intermediate concentrations of C_i^w and $S_nC_{ni}^s$, followed by preparing the corrector form of Eqs. (26) and (27) as given below.

3.4. For dissolved chemicals

$$h\frac{(C_i^w)^{N+1} - (C_i^w)^{N+1/2}}{\Delta\tau} = (\mathrm{RHS}_i^c)^{N+1} - (\mathrm{RHS}_i^c)^N \quad (\text{if } (\mathrm{RHS}_i^c)^N \geq 0)$$

$$= (\mathrm{RHS}_i^c)^{N+1} - \frac{(\mathrm{RHS}_i^c)^N}{(C_i^w)^N}(C_i^w)^{N+1/2} \ (\text{if } (\mathrm{RHS}_i^c)^N < 0) \tag{44}$$

where

$$(\mathrm{RHS}_i^c) = \sum_{m=1}^{N_{rx}} (a_{mi} - b_{mi}) k_m^{rb} h \left[\prod_{j=1}^{N_c} (C_j^w)^{b_{mj}} - \frac{k_m^{rf}}{k_m^{rb}} \prod_{j=1}^{N_c} (C_j^w)^{a_{mj}} \right] + \left[M_i^{cw} + h k_i^{ab} p_i + \sum_{n=1}^{N_s} k_{ni}^{sb} h (S_n C_{ni}^s) + \sum_{n=1}^{N_s} k_{ni}^{bb} (M_n C_{ni}^b) + M_i^{crw} + \sum_{n=1}^{N_s} \frac{R_n}{\rho_n} \theta_n C_i^{bw} \right] - \left[\lambda_i^w h + h k_i^{af} + \sum_{n=1}^{N_s} S_n h k_{ni}^{sf} + \sum_{n=1}^{N_s} M_n k_{ni}^{bf} + S + E + \sum_{n=1}^{N_s} \frac{D_n}{\rho_n} \theta_n \right] C_i^w \quad (45)$$

3.5. For particulate chemicals on suspended sediments

$$h \frac{(S_n C_{ni}^s)^{N+1} - (S_n C_{ni}^s)^{N+1/2}}{\Delta \tau} = (\mathrm{RHS}_{ni}^s)^{N+1} - (\mathrm{RHS}_{ni}^s)^N \quad (\text{if } (\mathrm{RHS}_{ni}^s)^N \geq 0)$$

$$= (\mathrm{RHS}_{ni}^s)^{N+1} - \frac{(\mathrm{RHS}_{ni}^s)^N}{(C_{ni}^s)^N} (C_{ni}^s)^{N+1/2} \quad (\text{if} (\mathrm{RHS}_{ni}^s)^N < 0) \quad (46)$$

where

$$(\mathrm{RHS}_{ni}^s) = \left[M_{ni}^{cs} + k_{ni}^{sf} h S_n C_i^w + \frac{R_n}{M_n} (M_n C_{ni}^b) - \frac{D_n}{S_n} (S_n C_{ni}^s) \right] - \left[\lambda_{ni}^s h + k_{ni}^{sb} h + S \right] (S_n C_{ni}^s) \quad (47)$$

Eqs. (5) and (6) can be written as follows.

3.6. For particulate chemicals on bed sediments

$$\frac{(M_n C_{ni}^b)^{N+1} - (M_n C_{ni}^b)^N}{\Delta t} = (\mathrm{RHS}_{ni}^b)^{N+1} \quad (48)$$

where

$$(\mathrm{RHS}_{ni}^b) = \left[\frac{D_n}{S_n} (S_n C_{ni}^s) - \frac{R_n}{M_n} (M_n C_{ni}^b) + k_{ni}^{bf} M_n C_i^w + k_{ni}^{2f} M_n C_i^{bw} \right] - \left[\lambda_{ni}^b + k_{ni}^{bb} + k_{ni}^{2b} \right] (M_n C_{ni}^b) \quad (49)$$

3.7. For dissolved chemicals in interstitial water of bed sediments

$$\frac{\left(\sum_{n=1}^{N_s} \frac{\theta_n}{\rho_n} M_n C_i^{bw} \right)^{N+1} - \left(\sum_{n=1}^{N_s} \frac{\theta_n}{\rho_n} M_n C_i^{bw} \right)^N}{\Delta t} = (\mathrm{RHS}_i^{bw})^{N+1} \quad (50)$$

where

$$(\mathrm{RHS}_i^{bw}) = \sum_{n=1}^{N_s} k_{ni}^{2b} M_n C_{ni}^b - \left(E + \sum_{n=1}^{N_s} \frac{D_n}{\rho_n} \theta_n + \sum_{n=1}^{N_s} k_{ni}^{2f} M_n \right) C_i^{bw} + \left(E + \sum_{n=1}^{N_s} \frac{D_n}{\rho_n} \theta_n \right) C_i^w + \left(\sum_{n=1}^{N_s} \frac{\theta_n}{\rho_n} M_n \right) \sum_{m=1}^{N_{rx}} (a_{mi} - b_{mi}) \times k_m^{rb} \left[\prod_{j=1}^{N_c} \left(C_j^{bw} \right)^{b_{mj}} - \frac{k_m^{rf}}{k_m^{rb}} \prod_{j=1}^{N_c} \left(C_j^{bw} \right)^{a_{mj}} \right] \quad (51)$$

Finally, we solve Eqs. (44), (46), (48) and (50) node-by-node with the Newton–Raphson method. When the

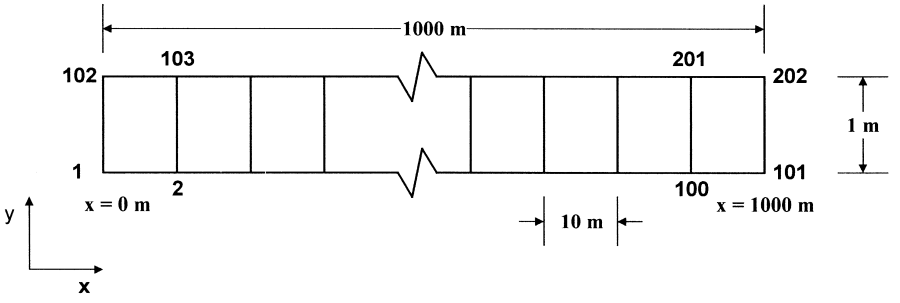

Fig. 2. The domain and its discretization of Example 1.

chemistry system is highly non-linear, we may have Jacobian entries vary over many orders of magnitude, which will introduce numerical difficulty in reaching correct solutions (Press et al., 1992). To overcome this, we incorporate full pivoting with a direct solver to correctly solve the Jacobian matrix equation resulting from the Newton–Raphson method (Yeh et al., 1998). The details of the residual equations and the associated Jacobian matrix for the Newton–Raphson method are given in the appendix of this paper. It is noted that when reaction rates are described with empirical formulae and the entries of the Jacobian matrix cannot be analytically derived as shown in the appendix, a numerical approach will be employed to determine the desired concentration derivatives.

4. Verification and demonstration

Verification has been made with several designed example problems, though not all given here, to determine the correctness of the numerical formulation and computer coding. In Example 1 below, we verify our model with the consumption of dissolved oxygen (**DO**), due to the release of organic waste, in a one-dimensional stream where a uniform flow is applied and thus the steady-state analytical solution is available. In addition to verification, we will examine how **DO** is influenced by other factors, such as diffusion, the volatilization of organic waste, the exchange between the column and the interstitial waters, and the sorption onto the bed sediment through numerical simulations. To demonstrate the model's ability to handle complicated problems, we consider a hypothetical problem involving the transport in San Diego South Bay subject to a semidiurnal tide in Example 2.

4.1. Example 1. One-dimensional *TOW / DO* transport subject to uniform flow

In this example we examine the transport of **DO**, total organic waste (**TOW**), and the residual from degradation (**RS**) under one-dimensional uniform flow of 10 m/min. The domain is 1000 m long and 2 m wide. A uniform water depth of 2 m is assumed throughout the entire domain. The domain is discretized with 100 elements and 202 nodes (Fig. 2) for a simulation run of

Table 1
List of simulation parameters for Example 1[a]

Parameters/cases	Case 1a	Case 1b	Case 1c	Case 1d	Case 2a	Case 3a
K_f^1 (1/min)	4.8×10^{-2}	9.6×10^{-3}	9.6×10^{-3}	9.6×10^{-3}	4.8×10^{-2}	4.8×10^{-2}
K_b^1 (kg/atm/m^3/min)	2.4×10^{-3}	4.8×10^{-4}	4.8×10^{-4}	4.8×10^{-4}	2.4×10^{-3}	2.4×10^{-3}
K_f^2 (1/min)	0	0	0	0	4.8×10^{-2}	0
K_b^2 (kg/atm/m^3/min)	0	0	0	0	0	0
K_b^4, k_b^{12} (1/min)	-1.2×10^{-2}	-1.2×10^{-2}	-3×10^{-3}	-2.4×10^{-2}	-1.2×10^{-2}	-1.2×10^{-2}
K_f^5, k_L^{13} (1/min)	2.4×10^{-2}	2.4×10^{-2}	6×10^{-3}	4.8×10^{-2}	2.4×10^{-2}	2.4×10^{-2}
K_f^6, k_f^7, k_f^8, k_f^9, k_f^{10}, k_f^{11} (1/min)	0	0	0	0	0	0
K_b^6, k_b^7, k_b^8, k_b^9, k_b^{10}, k_b^{11} (kg/m^3/min)	0	0	0	0	0	0
Diffusion coefficient (m^2/min)	0	0	0	0	0	0
E (m^3/m^2/min)[a]	0	0	0	0	0	1

Table 1 (*Continued*)

Parameters/cases	Case 3b	Case 4a	Case 4b	Case 5a	Case 5b	Case 6a
K_f^1 (1/min)	4.8×10^{-2}	4.8×10^{-2}	4.8×10^{-2}	4.8×10^{-2}	4.8×10^{-2}	4.8×10^{-2}
K_b^1 (kg/atm/m^3/min)	2.4×10^{-3}	2.4×10^{-3}	2.4×10^{-3}	2.4×10^{-3}	2.4×10^{-3}	2.4×10^{-3}
K_f^2 (1/min)	0	0	0	0	0	0
K_b^2 (kg/atm/m^3/min)	0	0	0	0	0	0
K_b^4, k_b^{12} (1/min)	-1.2×10^{-2}	-1.2×10^{-2}	-1.2×10^{-2}	-1.2×10^{-2}	-1.2×10^{-2}	-1.2×10^{-2}
K_f^5, k_L^{13} (1/min)	2.4×10^{-2}	2.4×10^{-2}	2.4×10^{-2}	2.4×10^{-2}	2.4×10^{-2}	2.4×10^{-2}
K_f^6, k_f^7, k_f^8, k_f^9, k_f^{10}, k_f^{11} (1/min)	0	0	0	2.0×10^{-3}	1.0×10^{-3}	2.0×10^{-3}
k_b^9, k_b^{10}, k_b^{11} (kg/m^3/min)	0	0	0	2.0×10^{-3}	1.0×10^{-3}	2.0×10^{-3}
Diffusion coefficient (m^2/min)	0	1	2	0	0	2
E (m^3/m^2/min)[a]	0.001	0	0	0	0	1

[a] Exchange coefficient between the column and the interstitial waters.

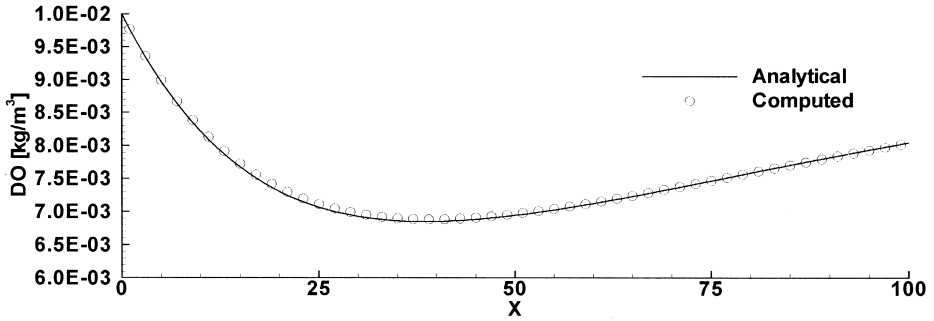

Fig. 3. The comparison of the concentration distribution of **DO** between the analytical solution and the computed result from our model for Case 1a.

150 min, where a constant time interval of 1 min is applied. **TOW** is assumed to degrade, due to the reaction with **DO**, with a first-order decay (Hemond and Fechner, 1994, pp. 109–111). The reaction can be expressed as

$$\mathbf{TOW} + \mathbf{DO} \rightarrow \mathbf{RS} \tag{52}$$

where the observed reaction rate R is

$$R = -\frac{\mathrm{d}[\mathbf{TOW}]}{\mathrm{d}t} = -\frac{\mathrm{d}[\mathbf{DO}]}{\mathrm{d}t} = \frac{\mathrm{d}[\mathbf{RS}]}{\mathrm{d}t} = \lambda[\mathbf{TOW}] \tag{53}$$

DO, **TOW**, and **RS** can be sorbed onto sediments to form particulate chemicals, where linear sorption kinetics (Saiers and Hornberger, 1996) is assumed. In other words, the sorption reaction can be written as

$$\mathbf{M} + \mathbf{S} \rightleftarrows \mathbf{M^S} + \mathbf{S} \qquad k_f, k_b \tag{54}$$

where **M** can be **DO**, **TOW**, or **RS**; **S** can be either a suspended or a bed sediment; $\mathbf{M^S}$ represents the particulate chemical of **M** sorbed on **S**; k_f and k_b are the forward and the backward rate constants of the sorption reaction. Thus, the rate change of the concentration of **M** can be expressed as follows.

$$\frac{\mathrm{d}[\mathbf{M}]}{\mathrm{d}t} = k_b[\mathbf{M^S}][\mathbf{S}] - k_f[\mathbf{M}][\mathbf{S}] \tag{55}$$

It is obvious that when equilibrium is reached, we have the rate change equal zero and the so-called distribution coefficient (i.e. K_d, the ratio of the sorbed concentration to the dissolved concentration at equilibrium) is equal to k_f/k_b.

By treating **DO**, **TOW**, and **RS** as three chemical species and assuming suspended sediments in the system are negligible under the given flow condition, we have three dissolved species in the water column (i.e. **DO**, **TOW**, and **RS**) as well as in the interstitial water (i.e. $\mathbf{DO^I}$, $\mathbf{TOW^I}$, and $\mathbf{RS^I}$), and three particulate chemicals sorbed on the bed sediment (i.e. $\mathbf{DO^B}$, $\mathbf{TOW^B}$, and $\mathbf{RS^B}$). In total, one bed sediment (**BS**) and nine chemical species are taken into account. The chemical reactions included in the system as stated above can be described as follows.

$$\mathbf{DO} \rightleftarrows \mathbf{P_{oxygen}} \quad k_f^1, k_b^1 \tag{R1}$$

$$\mathbf{TOW} \rightleftarrows \mathbf{P_{TOW}} \quad k_f^2, k_b^2 \tag{R2}$$

$$\mathbf{RS} \rightleftarrows \mathbf{P_{RS}} \quad k_f^3, k_b^3 \tag{R3}$$

$$\mathbf{DO} \rightleftarrows \mathbf{TOW} \quad k_f^4, k_b^4 \tag{R4}$$

$$\mathbf{TOW} \rightleftarrows \frac{1}{2}\mathbf{RS} \quad k_f^5, k_b^5 \tag{R5}$$

$$\mathbf{DO} + \mathbf{BS} \rightleftarrows \mathbf{DO^B} + \mathbf{BS} \quad k_f^6, k_b^6 \tag{R6}$$

$$\mathbf{TOW} + \mathbf{BS} \rightleftarrows \mathbf{TOW^B} + \mathbf{BS} \quad k_f^7, k_b^7 \tag{R7}$$

$$\mathbf{RS} + \mathbf{BS} \rightleftarrows \mathbf{RS^B} + \mathbf{BS} \quad k_f^8, k_b^8 \tag{R8}$$

$$\mathbf{DO^I} + \mathbf{BS} \rightleftarrows \mathbf{DO^B} + \mathbf{BS} \quad k_f^9, k_b^9 \tag{R9}$$

$$\mathbf{TOW^I} + \mathbf{BS} \rightleftarrows \mathbf{TOW^B} + \mathbf{BS} \quad k_f^{10}, k_b^{10} \tag{R10}$$

$$\mathbf{RS^I} + \mathbf{BS} \rightleftarrows \mathbf{RS^B} + \mathbf{BS} \quad k_f^{11}, k_b^{11} \tag{R11}$$

$$\mathbf{DO^I} \rightleftarrows \mathbf{TOW^I} \quad k_f^{12}, k_b^{12} \tag{R12}$$

$$\mathbf{TOW^I} \rightleftarrows \frac{1}{2}\mathbf{RS^I} \quad k_f^{13}, k_b^{13} \tag{R13}$$

where Eqs. (R1), (R2) and (R3) represent air–water chemical exchange reactions; Eqs. (R4) and (R5) represent the degradation of **TOW** in the water column; Eqs. (R12) and (R13) represent the degradation of **TOW** in the interstitial water; Eqs. (R6), (R7) and (R8) and Eqs. (R9), (R10) and (R11) represent the sorption reactions from the water column and from the interstitial water, respectively, onto the bed sediment; $\mathbf{P_{oxygen}}$, $\mathbf{P_{TOW}}$, and $\mathbf{P_{RS}}$ are assumed to be 0.2, 0, and 0 atm, respectively, representing the partial pressures of oxygen, **TOW**, and **RS** in the atmosphere; k_f^i and k_b^i represent the forward and the backward reaction rate constants, respectively, of the *i*-th reaction. All 13 reactions are assumed to be elementary. It is noted that we use reactions in Eqs. (R4) and (R5) and in Eqs. (R12) and (R13) to represent the **TOW** degradation as given in Eqs. (52) and (53) to match the reaction format in our model, where we define $k_f^4 = k_b^5 = k_f^{12} = k_b^{13} = 0$ and $k_f^5 = -2k_b^4 = k_f^{13} = -2k_b^{12} = 2\ \lambda$. In this example, we assume **RS** is not volatile, thus we have $k_f^3 = k_b^3 = 0$.

Initially, we have **DO** of 1×10^{-2} kg/m^3, which is in equilibrium with oxygen in the atmosphere, and the bed sediment of 50 kg/m^2 uniformly distributed throughout the domain. As the simulation begins, we have **TOW** of 2×10^{-2} kg/m^3 come into the domain through the left boundary side at $x = 0$ m. This setup

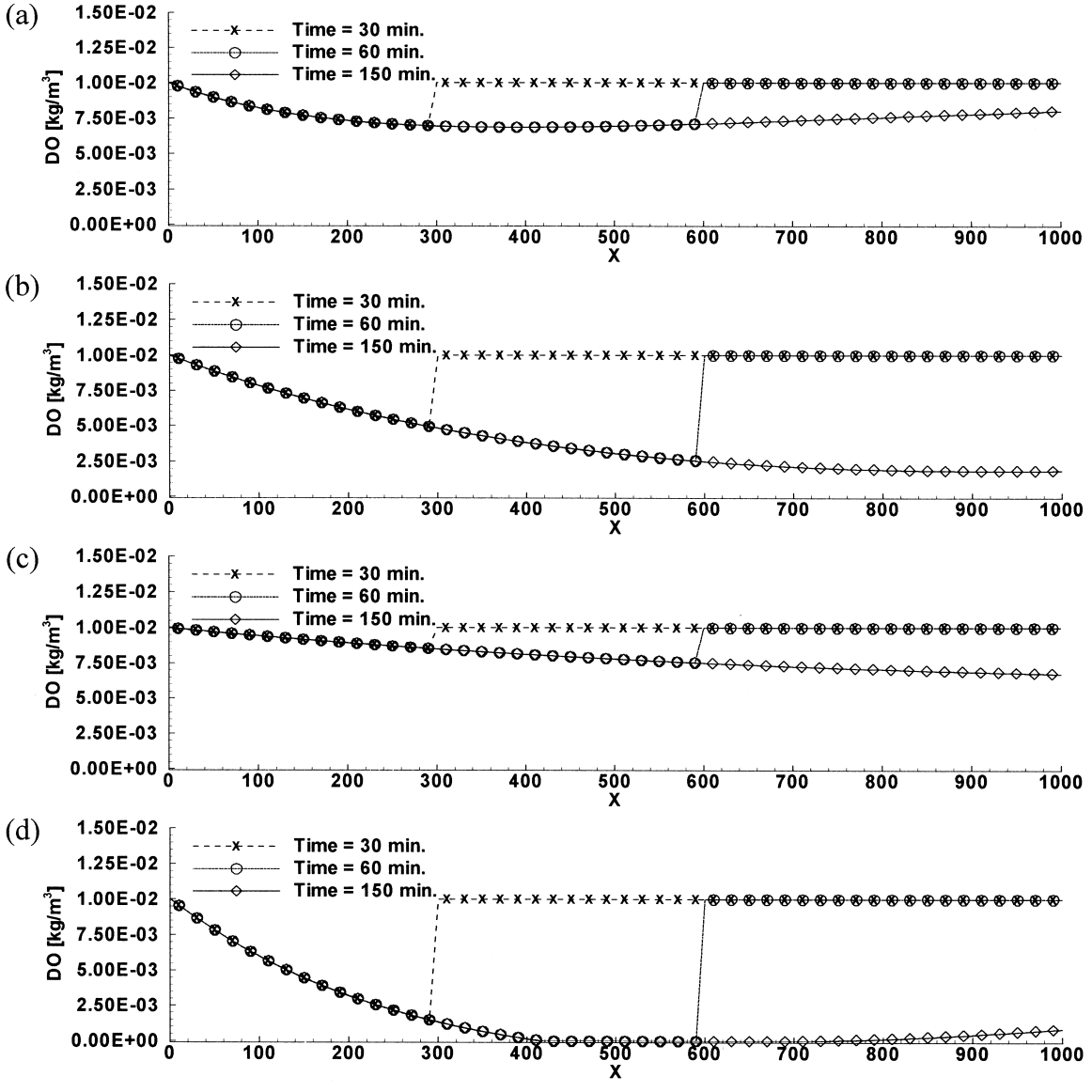

Fig. 4. The concentration distributions of **DO** at three different times for (a) Case 1a; (b) Case 1b; (c) Case 1c; and (d) Case 1d.

allows us to show how an outfall of **TOW** will change the concentration of **DO** in a one-dimensional uniform stream. The bulk density and porosity of the bed sediment are 1300 and 0.4 kg/m^3, respectively. The allowed maximum relative error of concentration is set to 10^{-4} for determining convergence. Table 1 lists a number of sets of simulation parameters used to examine the influence on chemical transport of the reaeration and degradation rates (Cases 1a through 2a), the exchange rate between the column and the interstitial waters (Cases 3a and 3b), the diffusion in the water column (Cases 4a and 4b), the sorption rate (Cases 5a and 5b), and a combination of all of the above.

Fig. 3 compares the numerical result of Case 1a with the corresponding analytical solution (Hemond and Fechner, 1994) at steady state, which serves as an example to verify our model. The results from Cases 1a–d demonstrate that the consumption of **DO** increases with decreasing reaeration rate (Fig. 4a,b) and increasing degradation rate of **TOW** (Fig. 4b–d). It is noted that there exists a section in which the concentration of **DO** is zero (i.e. from $X = 430$ to 750 in Fig. 4d). This may violate the assumption that there is enough **DO** for **TOW** to degrade such that the first-order decay can be applied. To avoid such a violation, the constraint associated with each assumption must be taken into account in constructing the numerical model. When **TOW** is volatile, i.e. the reaeration of **TOW** exists (Case 2a), the consumption of **DO** decreases (Fig. 5).

The numerical results of Cases 3a–4b show that both the diffusion of **DO** in the water column and the exchange between the interstitial water and the water in the water column can smoothen the depletion front of **DO** concentration. The larger the exchange coefficient (i.e. E in Table 1) and the diffusion coefficient, the smoother the formation of the depletion front (Fig. 6). It is also observed that the influences of diffusion and exchange on the steady-state concentration distribution are negligible in this advection–dominant example problem (the lines of time = 150 min in Fig. 6).

Fig. 7 demonstrates that although k_f/k_b for all sorption/desorption reactions are identical in Cases 5a and 5b, the consumption of **DO** decreases with increasing sorption rate when linear sorption kinetics is applied. This pinpoints the necessity of treating a reaction as kinetically controlled in any reactive transport system when the rate of concentration change due to chemical reaction is slow relative to that induced by water flux (Yeh et al., 1998).

In Case 6a, we combine Cases 3a, 4b, and 5a to examine the overall effect due to diffusion, exchange, and sorption. It is interesting to notice that the concentration distribution of **DO** at time = 150 min for this case (Fig. 8) has a variation trend similar to those of other cases considered in this example. Therefore, it is possible to adjust the sorption rate constants in Case 5a for obtaining a **DO** concentration profile matching that from Case 6a (e.g. using the least square error concept to perform curve fitting). However, the adjusted sorption rate constants are not true rate constants for the respective sorption/desorption reactions and will produce false results when the flow condition changes. In reactive transport modeling, we should

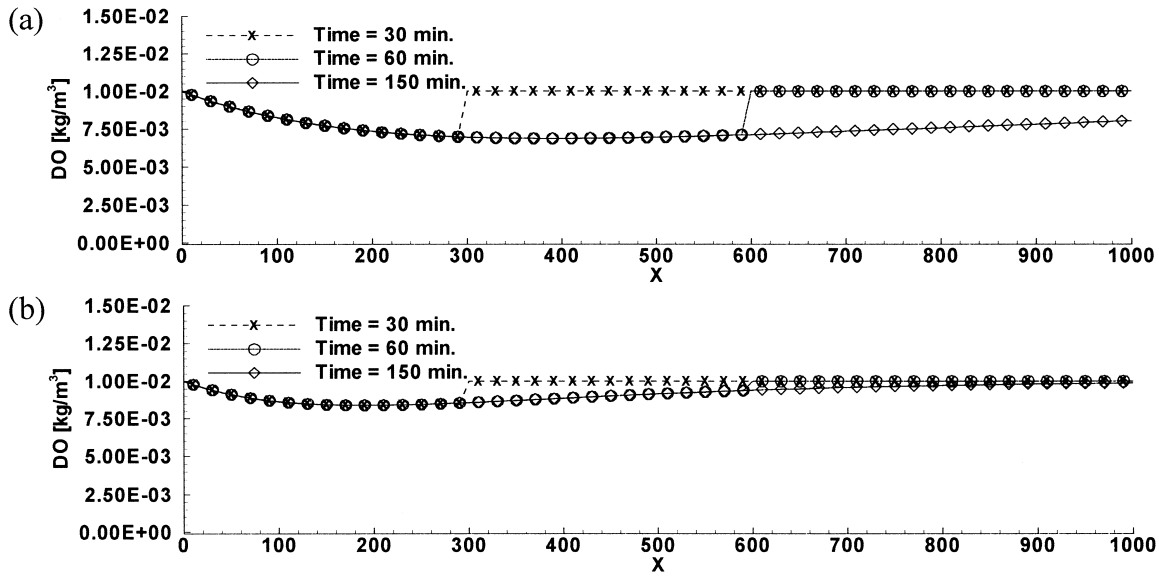

Fig. 5. The concentration distributions of **DO** at three different times for (a) Case 1a; and (b) Case 2a.

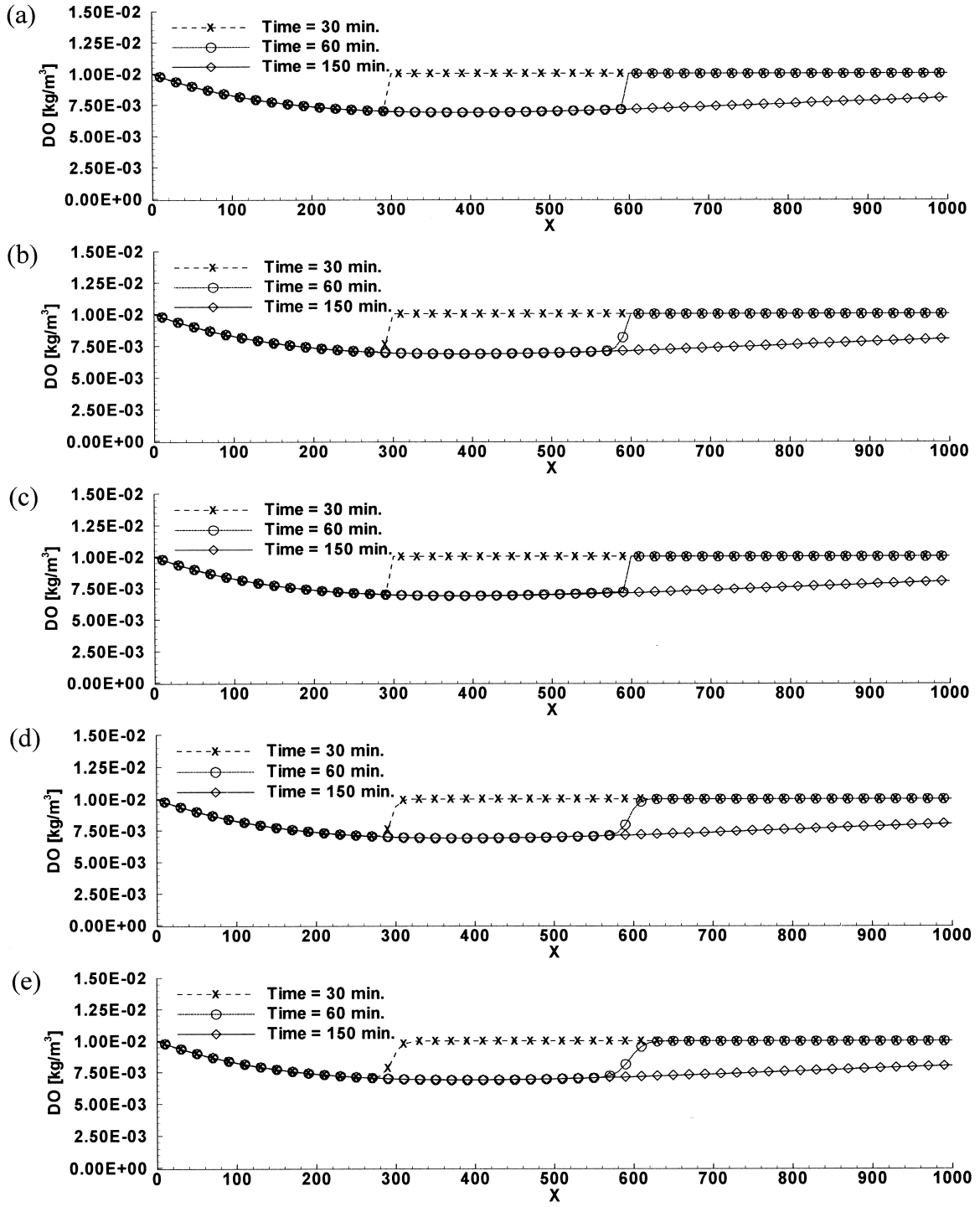

Fig. 6. The concentration distributions of **DO** at three different times for (a) Case 1a; (b) Case 3a; (c) Case 3b; (d) Case 4a; and (e) Case 4b.

always present a system in terms of its fundamental processes (i.e. the mechanistic approach). Otherwise, the system parameters are not intrinsic and will be applicable only for the condition under which the parameters were determined.

One other thing to be noted is that although the

observed rate equation [i.e. Eq. (53)] does not directly match the rate expression given in our model [i.e. Eq. (8)], it still can be correctly described in the model after some manipulation [i.e. using Eqs. (R4), (R5), (R12) and (R13)]. This is because a generally more sophisticated approach is capable of presenting a simpler approach in many cases. Thus, more of a system's important processes can be studied with the sophisticated approach.

Based on the conservation law, we can check the mass balance of **TOW** with the following relationship.

Change of [total TOW + total RS] in Δt

= Inflow of TOW in Δt − Outflow of [TOW + RS] in Δt

where **total TOW** includes **TOW**, $\mathbf{TOW^B}$, and $\mathbf{TOW^I}$; **total RS** includes **RS,** $\mathbf{RS^B}$, and $\mathbf{RS^I}$. The numerical results (Table 2) show that our model conserves mass for this one-dimensional problem precisely, which also verifies the model from another aspect.

4.2. Example 2. Transport in San Diego South Bay subject to a semidiurnal tide

In this example, we use our model to simulate the hypothetical transport of **DO**, **TOW**, and **RS**, as defined in Example 1, at San Diego South bay under a quasi-steady flow pattern determined according to an assumed semidiurnal tide. This quasi-steady flow pattern is computed by a hydrodynamic flow model which solves shallow water equations with the method of characteristics (Cheng et al., 1998a). The domain is discretized with 1415 elements and 1567 nodes (Fig. 9). The mean depth varies from 20 m near the ocean boundary to approximately 0.4 m toward the south end of the bay. The flow pattern is determined with a tidal boundary condition implemented on the ocean boundary side where the maximum tidal amplitude is 1.2 m and with the rest of the boundary treated as closed (Fig. 9). It is also assumed to be subject to eight point sources (Fig. 9), each with an injection rate of 1 m^3/s. Fig. 10 depicts

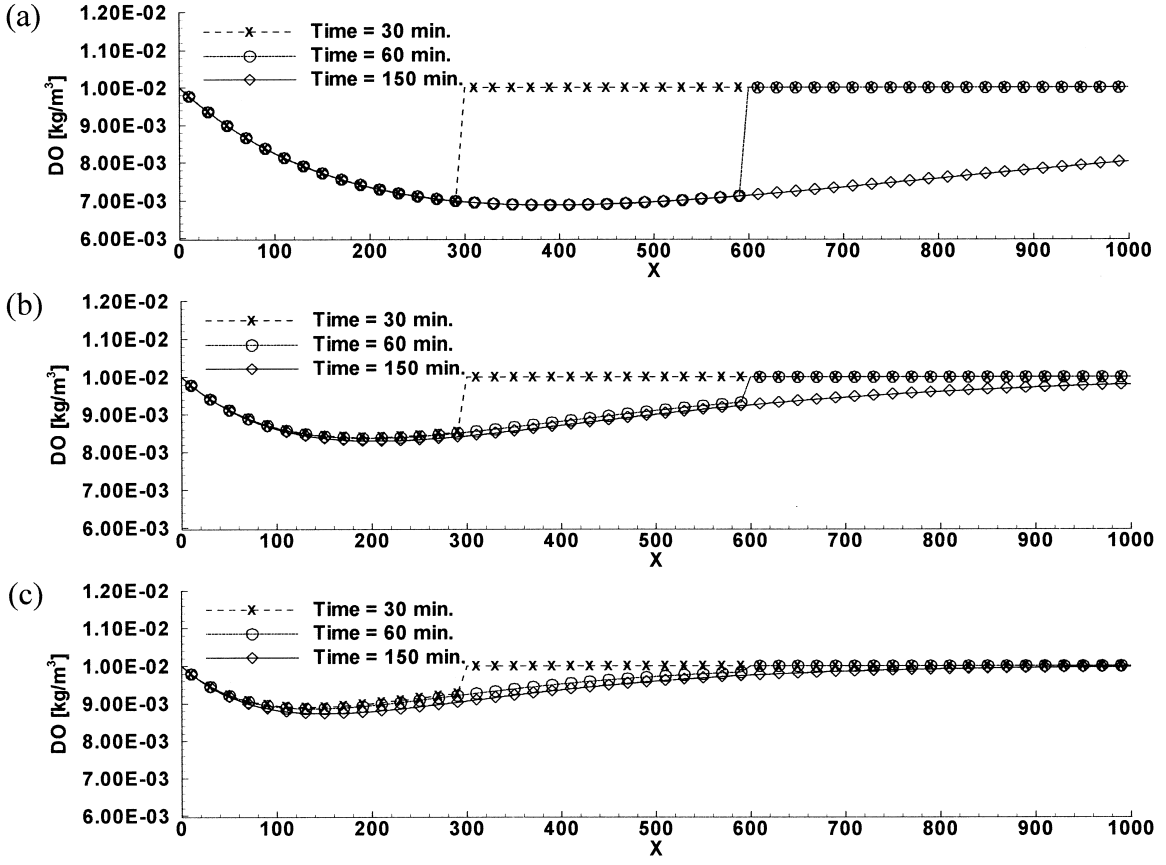

Fig. 7. The concentration distributions of **DO** at three different times for (a) Case 1a; (b) Case 5b; and (c) Case 5a.

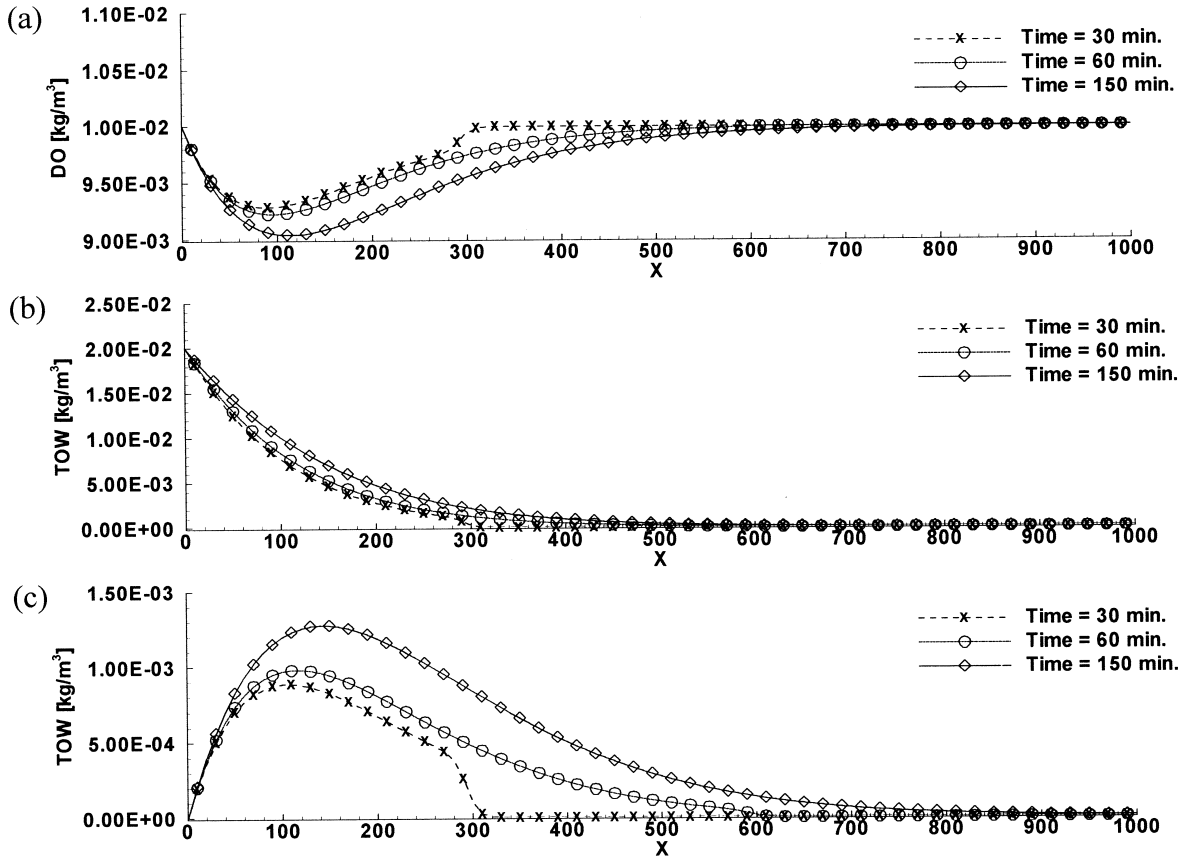

Fig. 8. The concentration distributions of (a) **DO**; (b) **TOW**; and (c) **RS** at three different times for Case 6a.

the contours of water surface elevation in the bay area at various times during one tidal cycle.

Table 2
Mass conservation error for cases in Example 1

Cases	Mass conservation error, ERR_{MC} (%)[a]	
	At time = 30 min	At time = 60 min
Case 1a	0	0
Case 1b	0	0
Case 1c	0	0
Case 1d	0	0
Case 3a	0	0
Case 3b	0	0
Case 4a[b]	0.034	0.017
Case 4b[b]	0.068	0.034
Case 5a	0	0
Case 5b	0	0
Case 6a	0	0

[a] $ERR_{MC} = |A - C|/A \times 100\%$, where A = analytical (total **TOW** + total **RS**) in the domain; and C = computed (total **TOW** + total **RS**) in the domain.

[b] The analytical mass used for Case 1a is taken as A in these cases.

It is assumed that during the simulation the amount of suspended sediments is negligible and a bed sediment with a bulk density of 1300 kg/m^3 and a porosity of 0.4 is uniformly distributed at a density of 100 kg/m^2 in the domain of interest. The same chemical reaction system, as defined with Eq. (R1) through Eq. (R13) in Example 1, is considered. In this example, both **TOW** and **RS** are assumed not volatile, i.e. $k_f^2 = k_f^3 = k_b^2 = k_b^3 = 0$, and **DO** and **TOW** are assumed not subject to sorption, i.e. $k_f^6 = k_f^7 = k_f^9 = k_f^{10} = k_b^6 = k_b^7 = k_b^9 = k_b^{10} = 0$.

Like that in Example 1, we have an initial **DO** of 1×10^{-2} kg/m^3 dissolved in the column and in the interstitial waters. As the simulation begins, the dissolved **TOW** of 2×10^{-1} kg/m^3 is released into the domain through eight point sources with an injection rate of 2×10^{-1} kg/s at each point source. Chemicals are neither radioactive nor volatile. The allowed maximum relative error of concentration is 10^{-4}. A 2-day simulation is performed with a constant time interval of 10 s. Table 3 lists some other simulation parameters used for this example.

Figs. 11 and 12 show the numerical results of the **DO**

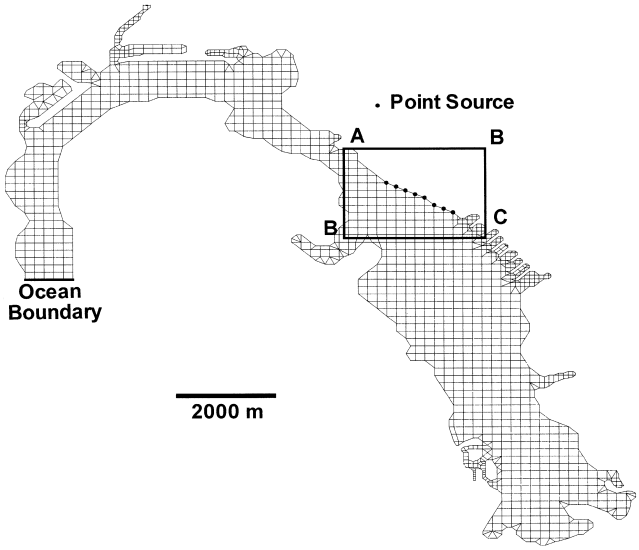

Fig. 9. The domain and its discretization of Example 2.

and **TOW** concentration distributions, respectively, for both cases given in Table 3 at time = 2 days. Since the two cases differ only in the sorption of **RS** onto the bed sediment and **RS** does not influence the degradation of **TOW**, the concentration distributions of **DO** and **TOW** are identical for both cases. It is also observed that the concentration change of **DO** and **TOW** is restricted in the region near the release of **TOW** (i.e. zone ABCD in Fig. 9). This is mainly because the degradation has restricted **TOW** from traveling far away from the release locations. On the other hand, however, **RS** can be transported a long distance (Fig. 13a) and make a significant environmental impact in the bay if it is continuously generated. The **RS** sorption by the bed sediment will retard the migration of **RS** (Fig. 13b) which would help delay the impact to the entire bay area so that remediation may be introduced in time to avoid any irreversible ecological damage.

It is well known that the LE approach does not conserve numerical mass mainly due to the decoupling process and the accumulated interpolation error when mesh Courant numbers are not integers in multi-dimensions (van Eijkeren, 1993; Gross et al., 1999). Gross et al. (1999) have demonstrated this elsewhere. However, this drawback can be alleviated by imposing adaptive local refinement and peak/valley capturing numerical techniques to keep the maximum computational error within the prescribed error tolerance (Cheng et al., 1996b, 1998b). As a result, the error associated with mass conservation can be ignored. Although such numerical techniques have not been incorporated into for the current version of the model, they will be implemented in a later version. As for the current version, finer grids will help reduce the interpolation error from the Lagrangian step.

5. Conclusions

We have presented a new approach to modeling reactive transport in two-dimensional shallow water domains which accounts for more reactions than have been included in previous models, hoping to more accurately simulate practical systems for environmental studies. Chemical reactions, including volatilization, aqueous complexation, and sorption/desorption, were assumed to be kinetically controlled, and reaction rates were computed through forward and backward reaction rate constants based on the collision theory. The set of reactive transport governing equations was solved with a predictor–corrector strategy when diffusion was not dominant. The Lagrangian–Eulerian finite element method and an adaptive explicit–implicit scheme were employed in the predictor step to assure non-negative concentration for each chemical, which is essential in chemical reaction modeling. The Newton–Raphson method was employed to solve the correction equations of reactive chemicals in the corrector step. An adaptive explicit–implicit scheme was applied to avoid negative numerical results. Two example problems considering the degradation of organic waste were used to partially verify the computer code, to demonstrate the capability of the model, and to point out the need for using a more mechanism-based approach in reactive transport modeling. The numerical approach of the model is

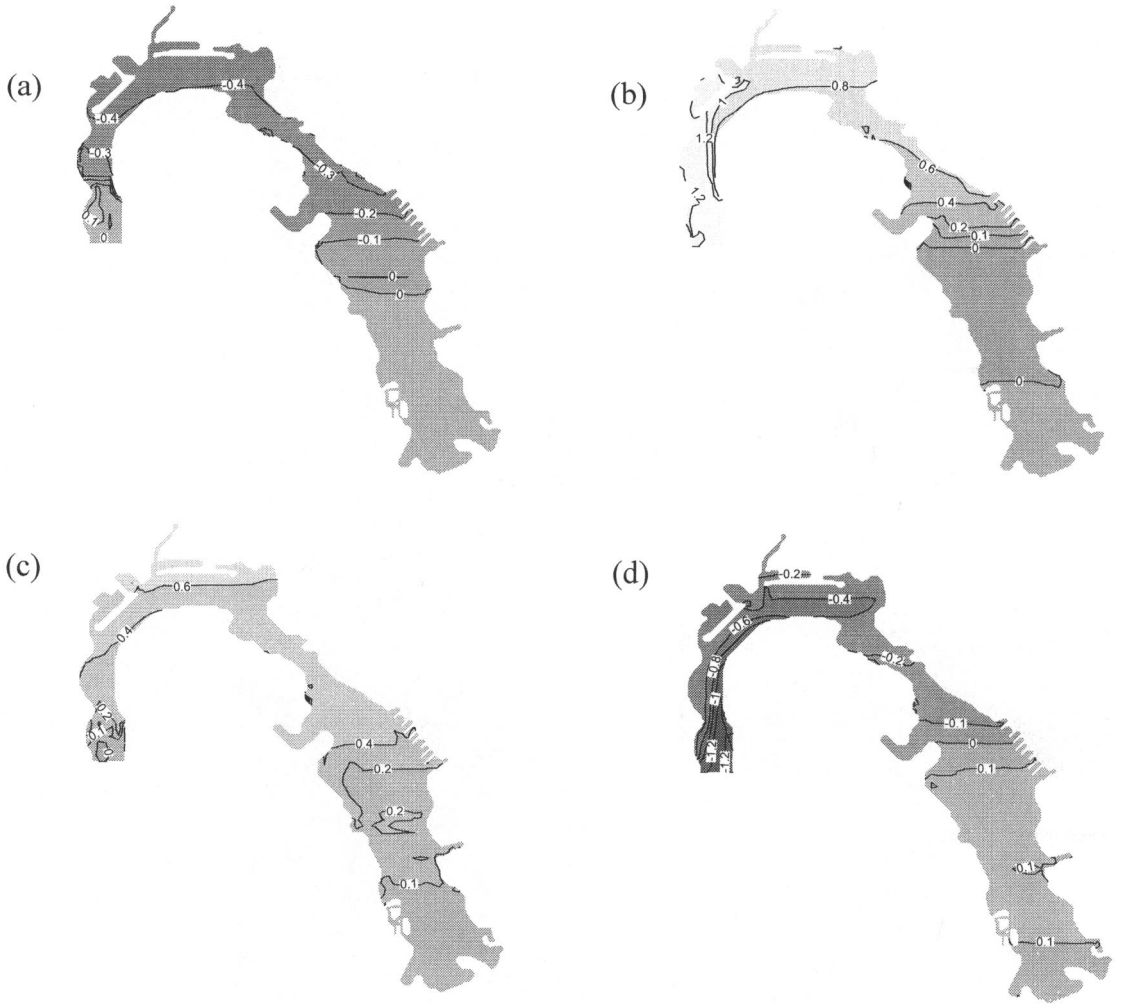

Fig. 10. Surface elevation at (a) 0 or T, (b) 0.25T, (c) 0.5T, and (d) 0.75T in the bay area during a tidal cycle where $T = 12$ h.

Table 3
List of simulation parameters for Example 2

Parameters/cases	Case 1	Case 2
K_f^1 (1/s)	1.6×10^{-4}	1.6×10^{-4}
K_b^1 (kg/atm/m^3/s)	8.0×10^{-6}	8.0×10^{-6}
K_b^4, k_b^{12} (1/s)	-2.0×10^{-4}	-2.0×10^{-4}
K_f^5, k_f^{13} (1/s)	4.0×10^{-4}	4.0×10^{-4}
K_f^8, k_f^{11} (1/s)	0	2.0×10^{-6}
K_b^8, k_b^{11} (kg/m^3/s)	0	2.0×10^{-6}
Diffusion coefficient (m^2/s)	0.1	0.1
E (m^3/m^2/s)[a]	1	1

[a] Exchange coefficient between the column and the interstitial waters.

robust for solving reactive transport equations and can be taken as a basis for further advancement.

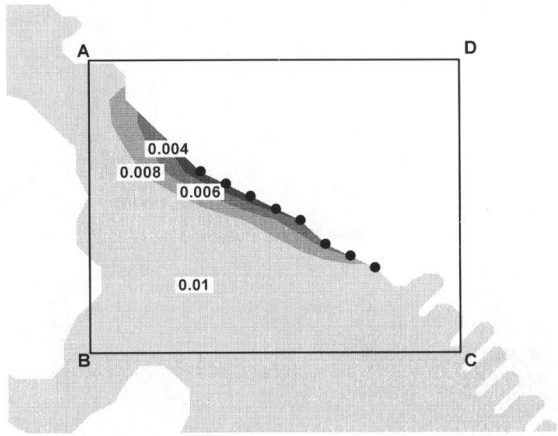

Fig. 11. The concentration distribution of **DO** [kg/m^3] at time = 2 days in both cases of Example 2.

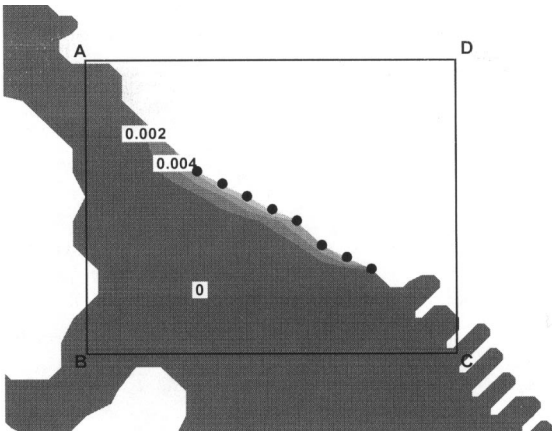

Fig. 12. The concentration distribution of **TOW** [kg/m^3] at time = 2 days in both cases of Example 2.

6. Nomenclature

NDs, number of sediment sizes;
$\mathbf{q}(x,y,t)$, flow flux $[L^2/T]$;
∇ del operator;
S_n, the depth-averaged sediment concentration of the n-th fraction size in the water column $[M/L^3]$;
$\mathbf{K}$, the dispersion coefficient tensor $[L^2/T]$;
M_n^s, the source of the n-th size fraction sediment $[M/L^2/T]$;
R_n, the erosion rate of the n-th size fraction sediment $[M/L^2/T]$;
D_n, the deposition rate of the n-th size fraction sediment $[M/L^2/T]$;
M_n, the sediment mass per unit horizontal bed area of the n-th size fraction $[M/L^2]$;
N_c, number of dissolved chemicals;
C_i^w, the depth-averaged concentration of the i-th dissolved chemical in the water column $[M/L^3]$;
M_i^{cw}, the source of the i-th dissolved chemical $[M/L^2/T]$;
λ_i^w, the combined first-order degradation rate constant of the i-th dissolved chemical $[1/T]$;
k_i^{ab}, k_i^{af}, the backward and the forward volatilization rate constants, respectively, associated with the i-th dissolved chemical in the atmosphere;
p_i, the partial pressure in the atmosphere associated with the i-th dissolved chemical [atm];
k_{ni}^{sb}, k_{ni}^{sf}, the backward and the forward sorption rate constants, respectively, associated with the i-th particulate chemical on suspended sediment of the n-th fraction size;
C_{ni}^b, the mass of particulate chemical on unit mass of bed sediment of the n-th fraction size $[M/M]$;
k_{ni}^{bb}, k_{ni}^{bf}, the backward and the forward sorption rate constants, respectively, associated with the i-th particulate chemical on bed sediment of the n-th fraction size;
C_{ni}^s, the mass of particulate chemical on unit mass of suspended sediment of the n-th fraction size $[M/M]$;
N_{rx}, number of aqueous complexation reactions;
k_m^{rb}, k_m^{rf}, the backward and the forward rate constants, respectively, of the m-th aqueous complexation reaction;
a_{mj} (b_{mj}), the stoichiometric coefficient of the j-th dissolved chemical in the m-th aqueous complexation reaction when this dis-

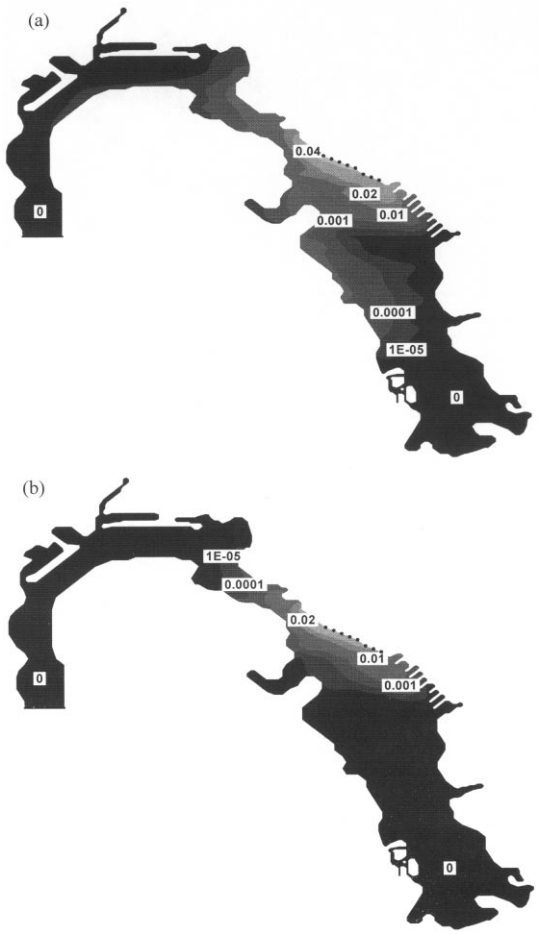

Fig. 13. The concentration distribution of **RS** [kg/m^3] at time = 2 days in (a) Case 1; and (b) Case 2 of Example 2.

solved chemical appears as a reactant (product) chemical;

C_i^{bw}, the concentration of the i-th dissolved chemical in the interstitial water $[M/L^3]$;

θ_n, the porosity of the n-th size fraction bed sediment;

ρ_n, the bulk density of the n-th size bed sediment $[M/L^3]$;

E, the volume exchange rate per unit area between the interstitial water in bed sediments and the water in the water column $[L^3/L^2/T]$;

M_{ni}^{cs}, the source of the i-th particulate chemical on suspended sediment of the n-th fraction size $[M/L^2/T]$;

λ_{ni}^{s}, the combined first-order degradation rate constant of the i-th particulate chemical on suspended sediment of the n-th fraction size $[1/T]$;

λ_{ni}^{b}, the combined first-order degradation rate constant of the i-th particulate chemical on bed sediment of the n-th fraction size $[1/T]$;

k_{ni}^{2b}, k_{ni}^{2f}, the backward and the forward sorption rate constants, respectively, associated with the i-th particulate chemical in the interstitial water of bed sediment of the n-th fraction size;

R_a, the rate of the aqueous complexation reaction;

R_{ad}^{s}, the rate of the sorption reaction between the water column and suspended sediments;

R_{ad}^{b1}, the rate of the sorption reaction between the water column and bed sediments;

R_{ad}^{b2}, the rate of the sorption reaction between the interstitial water and bed sediments;

R_v, the rate of the volatilization reaction;

$C_b(t)$, the prescribed time-dependent concentration on the boundary $[M/L^3]$;

$\mathbf{n}$, the outward unit normal vector of the boundary segment;

$C_{in}(t)$, the prescribed time-dependent concentration $[M/L^3]$, which is associated with the incoming flow;

$\mathbf{q}$, the flow flux vector $[L^2/T]$;

$\mathbf{K}$, the dispersion coefficient tensor$[L^2/T]$;

$C_o(t)$, the time-dependent concentration $[M/L^3]$ at the ocean boundary during the incoming flow;

$C_{\max}$, the maximum concentration at the end of the last outgoing flow;

f, the flushing decay constant;

$q_b^c(t)$, the prescribed time-dependent Cauchy flux $[M/T/L]$;

$q_b^n(t)$, the prescribed time-dependent Neumann flux $[M/T/L]$;

d/dt, the material or total derivative with respect to time;

η, the water surface elevation with respect to mean water level;

h, water depth $[L]$;

$V=(u,v)$, velocity $[L/T]$;

S, external source $[L/T]$;

Z_0, water bed elevation $[L]$;

d, water depth at mean water level $[L]$;

L, the dispersion operator,

$\Delta\tau$, time period consumed in backward particle tracking $[T]$;

Δt, time interval $[T]$;

C^*, the Lagrangian concentration $[M/L^3]$;

$(RHS)^N$, RHS evaluated at the previous time step $[M/L^2/T]$;

$C^{N+1/2}$, the intermediate concentration that we solve for with RHS evaluated at the previous time step $[M/L^3]$;

C^{N+1}, the concentration at the present time step $[M/L^3]$;

$(RHS)^{N+1}$, RHS evaluated at the present time step $[M/L^2/T]$;

w, time weighting factor;

$[QA]$, the mass matrix,

$[QD]$, the stiffness matrix due to dispersion;

$\{QR\}$, the load vector contributed from $(\mathrm{RHS})^N$;

$\{QB\}$, the load vector accounting for dispersive boundary fluxes;

R_e, the domain of element e;

B_e, the boundary of element e;

N_i^e, N_j^e, the element shape functions at the i-th and j-th element nodes, respectively, of element e;

$[QC]$, the stiffness matrix due to source/sink terms evaluated at the previous time step.

V_{sn}, the settling velocity of the n-th size fraction sediment $[L/T]$;

τ_{cDn}, the critical shear stress for the deposition of the n-th size fraction sediment $[\mathrm{M/L/T^2}]$;

τ_{cRn}, the critical shear stress for the erosion of the n-th size fraction sediment $[\mathrm{M/L/T^2}]$;

E_n, the erodibility of the n-th size fraction sediment $[M/L^2]$;

τ_b, the bottom shear stress or the bottom friction stress $[M/L/T^2]$;

Acknowledgements

This research was supported in part by the US National Shipbuilding Research Program Environmental Research Panel (NSRP SP-1) under contract with the Pennsylvania State University in the USA and in part by the ROC National Science Council under contract with National Tsing Hua University in Taiwan.

Appendix A

To achieve Step 3 in Section 4, the following residual equations are constructed, where we have $i \in [1, N_c]$ and $n \in [1, N_s]$ for the ranges of subscripts i and n.

For dissolved chemicals in the water column:

$$\begin{aligned}(\mathrm{RES}_i^c) &= h\left[(C_i^w)^{N+1} - (C_i^w)^{N+1/2}\right] \\ &\quad - \Delta\tau\left[(\mathrm{RHS}_i^c)^{N+1} - (\mathrm{RHS}_i^c)^N\right] \\ &\qquad (\text{if } (\mathrm{RHS}_i^c)^N \geq 0) \\ &= h\left[(C_i^w)^{N+1} - (C_i^w)^{N+1/2}\right] \\ &\quad - \Delta\tau\left[(\mathrm{RHS}_i^c)^{N+1} - \frac{(\mathrm{RHS}_i^c)^N}{(C_i^w)^N}(C_i^w)^{N+1/2}\right] \\ &\qquad (\text{if } (\mathrm{RHS}_i^c)^N < 0) \end{aligned} \tag{69}$$

For particulate chemicals on suspended sediments:

$$\begin{aligned}(\mathrm{RES}_{ni}^s) &= h\left[(S_n C_{ni}^s)^{N+1} - (S_n C_{ni}^s)^{N+1/2}\right] \\ &\quad - \Delta\tau\left[(\mathrm{RHS}_{ni}^s)^{N+1} - (\mathrm{RHS}_{ni}^s)^N\right] \\ &\qquad (\text{if } (\mathrm{RHS}_{ni}^s)^N \geq 0) \\ &= h\left[(S_n C_{ni}^s)^{N+1} - (S_n C_{ni}^s)^{N+1/2}\right] \\ &\quad - \Delta\tau\left[(\mathrm{RHS}_{ni}^s)^{N+1} - \frac{(\mathrm{RHS}_{ni}^s)^N}{(S_n C_{ni}^s)^N}(S_n C_{ni}^s)^{N+1/2}\right] \\ &\qquad (\text{if } (\mathrm{RHS}_{ni}^s)^N < 0) \end{aligned} \tag{70}$$

For particulate chemicals on bed sediments:

$$\begin{aligned}(\mathrm{RES}_{ni}^b) &= (M_n C_{ni}^b)^{N+1} - (M_n C_{ni}^b)^N \\ &\quad - \Delta t(\mathrm{RHS}_{ni}^b)^{N+1} \end{aligned} \tag{71}$$

For dissolved chemicals in the interstitial water of the bed sediments:

$$\begin{aligned}(\mathrm{RES}_i^{bw}) &= \left(\sum_{n=1}^{N_s} \frac{\theta_n}{\rho_n} M_n C_i^{bw}\right)^{N+1} - \left(\sum_{n=1}^{N_s} \frac{\theta_n}{\rho_n} M_n C_i^{bw}\right)^N \\ &\quad - \Delta t(\mathrm{RHS}_i^{bw})^{N+1} \end{aligned} \tag{72}$$

The entries of the associated Jacobian matrix are evaluated as follows.

For dissolved chemicals in the water column:

$$\begin{aligned}\frac{\partial(\mathrm{RES}_i^c)}{\partial(C_1^w)^{N+1}} &= \delta_{il} h + \delta_{il}\Delta\tau\left(\lambda_i^w h + SS + R + h k_i^{af}\right. \\ &\quad \left. + \sum_{n=1}^{N_s} S_n h k_{ni}^{sf} + \sum_{n=1}^{N_s} M_n k_{ni}^{bf} + E + \sum_{n=1}^{N_s} \frac{D_n}{\rho_n}\theta_n\right) \\ &\quad - \tau\left[\sum_{m=1}^{N_{rx}} (a_{mi} - b_{mi}) h\left(k_m^{rb} b_{ml} (C_1^w)_{ml}^{b-1}\right.\right. \\ &\quad \left.\left. \times \prod_{j=1, j\neq 1}^{N_c} (C_j^w)^{b_{mj}}\right)\right] \end{aligned} \tag{73}$$

$$\begin{aligned}&+ \Delta\tau\left[\sum_{m=1}^{N_{rx}} (a_{mi} - b_{mi}) h\left(k_m^{rf} a_{ml} (C_1^w)^{a_{ml}-1} \prod_{j=1, j\neq 1}^{N_c}\right.\right. \\ &\quad \left.\left. \times (C_j^w)^{a_{mj}}\right)\right] \end{aligned} \tag{74}$$

$$\frac{\partial(\mathrm{RES}_i^c)}{\partial(S_n C_{nl}^s)^{N+1}} = -\delta_{il}\Delta\tau k_{ni}^{sb} h \tag{75}$$

$$\frac{\partial(\mathrm{RES}_i^c)}{\partial(M_n C_{nl}^b)^{N+1}} = -\delta_{il}\Delta\tau k_{ni}^{bb} \tag{76}$$

$$\frac{\partial(\mathrm{RES}_i^c)}{\partial(C_1^{bw})^{N+1}} = -\delta_{il}\Delta\tau\left(E + \sum_{n=1}^{N_s} \frac{\theta_n}{\rho_n} R_n\right) \tag{77}$$

For particulate chemicals on suspended sediments:

$$\frac{\partial(\mathrm{RES}_{ni}^s)}{\partial(C_1^w)^{N+1}} = -\delta_{il}\Delta\tau k_{ni}^{sf} S_n h \tag{78}$$

$$\begin{aligned}\frac{\partial(\mathrm{RES}_{ni}^s)}{\partial(S_n C_{nl}^s)^{N+1}} &= \delta_{il} h + \delta_{il}\Delta\tau\frac{D_n}{S_n} + \delta_{il}\Delta\tau(\lambda_{ni}^s h + k_{ni}^{sb} h \\ &\quad + SS + R) \end{aligned} \tag{79}$$

$$\frac{\partial(\mathrm{RES}_{ni}^{s})}{\partial(M_n C_{nl}^{b})^{N+1}} = -\delta_{il}\Delta\tau\frac{R_n}{M_n} \tag{80}$$

$$\frac{\partial(\mathrm{RES}_{ni}^{s})}{\partial(C_{l}^{bw})^{N+1}} = 0 \tag{81}$$

For particulate chemicals on bed sediments:

$$\frac{\partial(\mathrm{RES}_{ni}^{b})}{\partial(C_{l}^{w})^{N+1}} = -\delta_{il}\Delta t k_{ni}^{bf} M_n \tag{82}$$

$$\frac{\partial(\mathrm{RES}_{ni}^{b})}{\partial(S_n C_{nl}^{s})^{N+1}} = -\delta_{il}\Delta t\frac{D_n}{S_n} \tag{83}$$

$$\frac{\partial(\mathrm{RES}_{ni}^{b})}{\partial(M_n C_{nl}^{b})^{N+1}} = \delta_{il} + \delta_{il}\Delta t\frac{R_n}{M_n} + \delta_{il}\Delta t \times(\lambda_{ni}^{b} + k_{ni}^{bb} + k_{ni}^{2b}) \tag{84}$$

$$\frac{\partial(\mathrm{RES}_{ni}^{b})}{\partial(C_{l}^{bw})^{N+1}} = -\delta_{il}\Delta t k_{ni}^{2f} M_n \tag{85}$$

For dissolved chemicals in the interstitial water of the bed sediments:

$$\frac{\partial(\mathrm{RES}_{i}^{bw})}{\partial(C_{l}^{w})^{N+1}} = -\delta_{il}\Delta t\left(E + \sum_{n=1}^{N_s}\frac{D_n}{\rho_n}\theta_n\right) \tag{86}$$

$$\frac{\partial(\mathrm{RES}_{i}^{bw})}{\partial(S_n C_{nl}^{s})^{N+1}} = 0 \tag{87}$$

$$\frac{\partial(\mathrm{RES}_{i}^{bw})}{\partial(M_n C_{nl}^{b})^{N+1}} = -\delta_{il}\Delta t k_{ni}^{2b} \tag{88}$$

$$\begin{aligned}\frac{\partial(\mathrm{RES}_{i}^{bw})}{\partial(C_{l}^{bw})^{N+1}} = {} & \delta_{il}\left(\sum_{n=1}^{N_s}\frac{\theta_n}{\rho_n}M_n\right) + \delta_{il}\Delta t\left(E + \sum_{n=1}^{N_s}\frac{D_n}{\rho_n}\theta_n + \sum_{n=1}^{N_s}k_{ni}^{2f}M_n\right) - \Delta t\left(\sum_{n=1}^{N_s}\frac{\theta_n}{\rho_n}M_n\right) \\ & \times\left[\sum_{m=1}^{N_{rx}}(a_{mi}-b_{mi})\left(k_m^{rb}b_{ml}(C_l^{bw})^{b-1_{ml}} \times\prod_{j=1,j\neq 1}^{N_c}\left(C_j^{bw}\right)^{b_{mj}} - k_m^{rf}a_{ml}(C_l^{bw})^{a_{ml}-1} \times\prod_{j=1,j\neq 1}^{N_c}\left(C_j^{bw}\right)^{a_{mj}}\right)\right]\end{aligned} \tag{89}$$

References

Blumberg, A.F., Ji, Z.-G., Ziegler, C.K., 1996. Modeling outfall plume behavior using far field circulation model. J. Hydraul. Eng. 122 (11), 610–615.

Cheng, H.P., Yeh, G.T., 1998. Development of a three-dimensional model of subsurface flow, heat transfer, and reactive chemical transport: 3 DHYDROGEOCHEM. J. Contam. Hydrol. 34, 47–83.

Cheng, H.P., Cheng, J.R., Yeh, G.T., 1996a. A particle tracking technique for the Lagrangian–Eulerian finite element method in multi-dimensions. Int. J. Numer. Methods Eng. 39 (7), 1115–1136.

Cheng, J.R., Cheng, H.P., Yeh, G.T., 1996b. A Lagrangian–Eulerian method with adaptively local zooming and peak/valley capturing approach to solve two-dimensional advection–diffusion transport equations. Int. J. Numer. Methods Eng. 39 (6), 987–1016.

Cheng, H.P., Cheng, J.R., Yeh, G.T., Lin, H.C., 1998a. Finite element modeling of free surface flow with MOC-diagonalized shallow water equations. Proceedings of the Tenth International Conference on Finite Elements in Fluids, pp. 375–380.

Cheng, H.P., Cheng, J.R., Yeh, G.T., 1998b. A Lagrangian–Eulerian method with adaptively local zooming and peak/valley capturing approach to solve three-dimensional advection–diffusion transport equations. Int. J. Numer. Methods Eng. 41 (4), 587–615.

Chilakapathi, A., 1995. A Simulator for Reactive Flow and Transport of Groundwater Contaminants. Report PNL-10636, Pacific Northwest Laboratory, USA.

Falconer, R.A., 1990. Engineering problems and the application of mathematical models relating to combating water pollution. Munic. Eng. 7 (6), 281–291.

Falconer, R.A., 1992. Flow and water-quality modelling in coastal and island waters. J. Hydraul. Res. 30, 437–452.

Falconer, R.A., Lin, B., 1997. Three-dimensional modelling of water quality in the Humber estuary. Water Res. 31 (5), 1092–1102.

Graf, W.H., 1984. Hydraulics of Sediment Transport. Water Resources Publication, p. 513.

Gross, E.S., J.R., Koseff, Monismith, S.G., 1999. Evaluation of advective schemes for estuarine salinity simulations, Journal of Hydraulic Engineering, 125 (1), 32–46.

Hinkelmann, R., Zielke, W., 1996. Parallel three-dimensional Lagrangian-Eularian model for the shallow water and transport equations, Proceedings for the 11th International Conference on Computational Methods in Water Resources, CMWR 96, v 2, 71–78.

Hemond, H.F., Fechner, E.J., 1994. Chemical Fate and Transport in the Environment, Academic Press.

McDonald, E.T., Cheng, R.T., 1994. Issues related to modelling the transport of suspended sediments in Northern San Francisco Bay, California, Proceedings of the 3rd International Conference of Estuarine and Coastal Modeling, 551–564.

Ors, H., 1997. Contaminant transport model for the Bosphorus Strait, Journal of Environmental Science and Health, Part A: Environmental Science and Engineering & Toxic and Hazardous Substance Control, 32 (3), 699–714.

Park, K., Kuo, A.Y., 1996. Multi-step computation scheme: decoupling kinetic processes from physical transport in water quality models, Water Research, 30 (10), 2255–2264.

Paulsen, S.C., Owen, R.M., 1996. Quantitative model of sediment dispersal and heavy mineral distribution in North Cardigan Bay, Irish Sea, Mirine Geosources and Geotechnology, 14 (2), 143–159.

Press, W.H., Teukolsky, S.A., Vetterling, W.T., Flannery, B.P., 1992. Numerical Recipes, 2nd edition, Cambridge, 963p.

Saiers, J.E., Hornberger, G.M., 1996. 'Migration of ^{137}Cs through quartz sand: experimental results and modeling approaches' Journal of Contaminant Hydrology, 22, 255–270.

Salvage, K.M., 1998. Reactive contaminant transport in variably saturated porous media: biogeochemical model development, verification, and application, Ph.D. thesis in Civil and Environmental Engineering, The Pennsylvania State University, USA.

Sheng, Y.P., Chen, X., Yassuda, E.A., 1995a. Wave-induced sediment resuspension and mixing in shallow waters, Proceedings of the 24th International Conference on Coastal Engineering, Part 3 (of 3), 3281–3294.

Sheng, Y.P., Yassuda, E.A., Yang, C., 1995b. Modeling the effect of reduced nitrogen loading on water quality, Proceedings of the 4th International Conference of Estuarine and Coastal Modeling, 644–658.

Sommeijer, B.P., Kok, J., 1996. Splitting methods for three-dimensional bio-chemical transport, Applied Numerical Mathematics, 21 (3), 303–320.

Spitaleri, R.M., Corinaldesi, L., 1997. Multigrid semi-implicit finite difference method for the two-dimensioanl shallow water equations, International Journal for Numerical Methods in Fluids, 25 (11), 1229–1240.

Steefel, C.I., Cappellen, P.V., 1998. Reactive transport modeling of natural systems (preface), Journal of Hydrology 209, 1–7.

Stumm, W., Morgan, J.J., 1981. Aquatic chemistry—an introduction emphasizing chemical equilibria in natural waters, John Wiley & Sons, 780 p.

van Eijkeren, J.C.H., 1993. Backward semi-Langrangian methods: an adjoint equation method, Numerical methods for advection-diffusion problems. In: C.B. Vreugdenhil, B. Koren (eds.), 45, Notes on numerical fluid mechanics, Chapter 9, Viewweg, Washington, D.C., 215–241.

Wang, J.D., Connor, J.J., 1975. Mathematical modeling of near coastal circulation, Report MITSG 75–13, Massachusetts Institute of Technology, MA, USA.

Wood, T.M., Baptista, A.M., 1992. Modelling the pathways of nonconservative substances in estuaries, Proceedings of the 2nd International Conference on Estuarine and Coastal Modeling, 280–291.

Yeh, G.T., 1990. A Langrangian-Eularian method with zoomable hidden fine-mesh approach to solving advection-dispersion equations, Water Resources Research, 26 (6), 1133–1144.

Yeh, G.T., Tripathi, V.S., 1990. HYDROGEOCHEM: A Coupled Model of HYDROlogical Transport and GEOCHEMical Equilibria in Reactive Multicomponent Systems, Report ORNL-6371, Oak Ridge National Laboratory, Oak Ridge, TN, USA.

Yeh, G.T., Chang, J.R., Short, T.E., 1992. An exact peak capturing and oscillation-free scheme to solve advection-dispersion transport equations, Water Resources Research, 28 (11), 2937–2951.

Yeh, G.T., Iskra, G., Zachara, J.M., Szecsödy, J.E., 1998. Development and verification of a mixed chemical kinetic and equilibrium model, Advances in Environmental Research, 2 (1), 24–56.